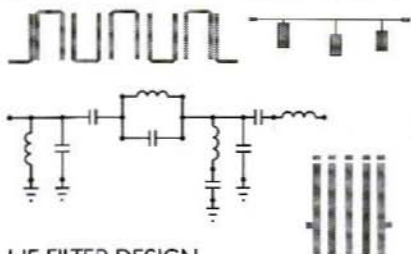


DESIGN OSCILLATORS & FILTERS



HF FILTER DESIGN AND COMPUTER SIMULATION

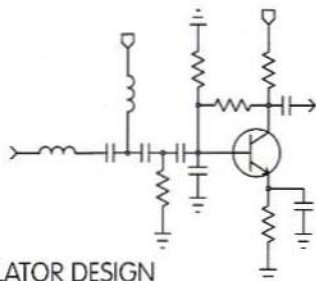
This book is packed with invaluable information on the practical design of L-C and distributed (both printed and machined) filters.

- ✓ Great collection of lumped and line models
- ✓ Simple, narrow and special bandpass
- ✓ Zig-zag and other elliptic types
- ✓ Equivalent circuit transformations
- ✓ End, edge and direct coupled
- ✓ Hairpin, combline and interdigital
- ✓ Group delay equalization
- ✓ Computer aided techniques
- ✓ Photographs and measured responses



428 Pages
180 Figures
62 Tables
301 Equations

\$59



OSCILLATOR DESIGN AND COMPUTER SIMULATION

Contains easy-to-understand oscillator theory and practical tips and techniques for L-C, transmission line, SAW and crystal oscillators. Some of the topics are:

- ✓ Easy-to-understand design goals
- ✓ L-C, π -line, crystal and SAW resonators
- ✓ Bipolar and JFET amplifiers
- ✓ Starting characteristics
- ✓ Noise performance
- ✓ VCOs
- ✓ Pulling crystal oscillators
- ✓ Linear and non-linear computer analysis
- ✓ Lots of examples



300 Pages
136 Figures
27 Tables
275 Equations

\$64

Name _____
Company _____
Address _____
City _____ State _____
ZIP _____ Country _____
Phone _____ FAX _____
Card # _____ Exp _____
Signature _____

Please send the following products

- Oscillator Design \$64
 HF Filter Design \$59
 Both Books \$99

Shipping & Handling
United States \$ 5
International Air \$20

Payment Method

- VISA or MASTERCARD
 EuroCheck
 Bank Check (Must have the name of a US bank on the check)

NOBLE PUBLISHING

2245 Dillard Street TEL (404)908-2320
Tucker, GA 30084 USA. FAX (404)939-0157



Contents

Matjaz Vidmar S53MV	A DIY Receiver for GPS and GLONASS Satellites Part-7 (conclusion)	194 - 205
Dipl.-Ing. Detlef Burchard	Linear Signal Rectification Part-2 (conclusion)	206 - 216
Harald Fleckner DC8UG	A 10 Watt Power Amplifier for the 13cm Band using GaAs Technology Developed with the help of PUFF CAD Software	217 - 228
Dr.Ing. Jochen Jirmann	New Software for the Digital Image Store for the DB1NV 010 Spectrum Analyser	229 - 230
Andreas Schaumburg DF7ZW	A Simple DC-to-DC Down Converter for Amateur Radio Applications	231 - 234
François Cronauer	First Amateur Cloud Scatter Beacon in Europe	235 - 239
Norbert Kohns DG1KPN	Digital Display for the Logarithmic Detector Amplifier from DJ4GC	240 - 245
Angel Vilaseca HB9SLV	The World's Smallest 10 GHz ATV Transmitter	246 - 252

We would like to wish you all a belated Happy and Prosperous New Year. Thank you for your past and continuing support of VHF Communications, without you it would not exist.

To our friends and subscribers in those parts of the world where the dawn of 1996 has offered the prospects of Peace and a New Beginning, we especially extend our warmest feelings and hopes.

Krystyna, Michael & Family - KM Publications



KM Publications, 5 Ware Orchard, Barby, Rugby, CV23 8UF, UK

Telephone: (0)1788 890365; INT: +44 1788 890 365; FAX: (0)1788 891883
INTERNET: vhf-comm@g6iqm.demon.co.uk COMPUSERVE: 100441,377
WWW <http://www.taynet.co.uk/~gdx/ag/vhfcomm.htm>



Matjaz Vidmar, S53MV

A DIY Receiver for GPS and GLONASS Satellites

Part-7 (conclusion)

In this the final part of this project the Receiver Software is described, detailing the Real-Time tasks, Main Program-Loop tasks and the Software Menus and Commands.

5. GPS & GLONASS RECEIVER SOFTWARE

5.1 GPS/GLONASS Receiver Software Overview

Satellite navigation is one of the first applications that totally depends on the availability of suitable computers and the corresponding software. Although initially the digital computer was only intended to solve the navigation equations, other tasks were being gradually added to simplify the hardware in front of and behind the computer itself. In the GPS/GLONASS receiver described

even most of the signal processing is performed in software, just to keep the analogue front-end and dedicated DSP hardware as simple as possible.

The software running in a GPS or GLONASS receiver is therefore very complex and includes a variety of very different functions. For example, digital signal processing requires quick but simple integer arithmetic, while solving the navigation equations requires high accuracy floating-point arithmetic. The latter does not need to be as quick as the former signal processing, but a considerable number of operations still need to be performed in a limited amount of time.

To make a fair comparison one should consider the development time for the hardware and for the software.

In the case of the navigation receiver described here, the software required between twice and three times as much time to develop than the hardware!



Unfortunately, it is much more difficult to describe the software down to the smallest detail than it is the hardware. For the hardware one can draw the circuit diagrams and prepare detailed parts lists. On the other hand, detailed descriptions of the software tend to become boring and minor details tend to hide the real problem being solved.

Therefore, only the major functions performed by the software will be described in this article. These include signal acquisition and processing, almanac and precision ephemeris data collection, time and frequency measurements, solving the navigation equations and data display in a suitable format for the user. At the end the user interface, display menus and user commands will be described in detail.

The overall software is written in different languages due to the differing functions to be performed: MC68010 assembly language, DSP computer high-level language and even directly in machine code.

The digital signal processing software is written in the MC68010 assembly language. The corresponding file has the extension .ASM. This file is first compiled into machine code and then into hexadecimal format, so that it can be easily inserted in the DSP computer high-level language.

The orbital mechanics and navigation equation part is written in the DSP computer high-level language. The latter supports a floating-point format with a 32-bit mantissa and 16-bit exponent. A 32-bit mantissa is generally sufficient considering the accuracy of the data obtained from the GPS or GLONASS

satellites. The corresponding file has an extension .SRC and can be compiled into a .EXE file and executed on a DSP computer equipped with the described dedicated DSP hardware board, but with an unmodified CPU board!

In a portable GPS/GLONASS receiver all of the software is stored in a 27C256 EPROM. The latter includes a starting program, the high-level language compiler and a version of the .SRC file with all of the comments and unnecessary symbols removed.

When the portable receiver is turned on the program is compiled in the RAM. This operation takes around 10 seconds and is necessary to save EPROM space, since the compiled program in the RAM takes around 100 kbytes.

The present discussion applies to the current software versions V122 (GPS) or V39 (GLONASS). When running the software on a DSP computer the type of display may be selected by the TOTAL/PARTIAL RESET switch while starting the program: switch open (TOTAL RESET) selects the LCD, while switch closed (PARTIAL RESET) selects the CRT display. Of course, the LCD can only be selected in a stand-alone portable receiver, and the corresponding input on the CPU board MUST BE LEFT OPEN!

5.2 Real-Time Tasks: Signal Acquisition and Processing

The signal acquisition and processing tasks run under the 1 kHz interrupts requested by the dedicated DSP hardware module.

The tasks include:

- Multiplexing of the single-channel hardware among four different satellites,
- C/A-code synchronisation acquisition and tracking,
- Carrier lock acquisition and tracking,
- The 50bps navigation-data demodulation,
- Bit synchronisation and frame synchronisation with parity check
- Averaging of the measured code phase, code rate and carrier frequency.

After an interrupt request is received from the dedicated DSP hardware, the interrupt-servicing routine will first latch the contents of all the counters in the dedicated hardware. It will then read the latched content and reset and arm the interrupt request flip-flop. The hardware counters are never reset. The actual integrated value is computed from the difference between the actual counter content and the previous sample content. The four differences are further normalised using the result from the reference 1ms divider. Finally, the interrupt-servicing routine also increments a 32-bit millisecond counter, which is later used to relate the measurements to the 50bps navigation data.

The single-channel hardware is multiplexed among all of the satellites received. However, due to the limitations of the hardware, switching to another satellite will corrupt one millisecond of data. Therefore, the basic

multiplexing period includes one millisecond to switch the hardware followed by 8 milliseconds to collect the data from a given satellite. After this 9 millisecond period the hardware is switched to another satellite. The multiplexing rate is therefore 111 hops per second.

The multiplexing rate and especially the multiplexing sequence have to be chosen carefully. The navigation data is transmitted at a speed of 50bps, so one bit is 20ms long and lasts exactly 20 interrupt periods. If the navigation data is to be collected from a given satellite, then this satellite should get at least a few 1ms samples of data from each 20ms bit period. Further, the multiplexing period should not be an integer submultiple of the bit period, so that the bit transitions can be detected.

Considering the limitations of the single-channel hardware, the multiplexing sequence can not allow the collecting of navigation data from more than two satellites at a time. In practice, since four satellites need to be received for a navigation solution, the navigation data can only be collected from a single satellite at a time using half of the single-channel hardware time. The remaining hardware time is split among the remaining three satellites. The privileged satellite that gets more hardware time of course needs to be periodically exchanged to allow collecting of the navigation data from all four satellites.

There is yet another constraint on the multiplexing sequence. If a certain satellite only gets a few sampling periods, then false locks of the carrier



recovery loop become very likely. In order to avoid this, the following multiplexing sequence is used in the GPS/GLONASS receivers in this project (1 = privileged satellite; 2, 3 & 4 = others):

121213141412131314

121213141412131314

...

The complete multiplexing sequence therefore repeats after 18 multiplexing periods or 162 milliseconds.

The C/A-code synchronisation is always obtained from the signal magnitude obtained from the dedicated hardware. The signal phase information is intentionally not used for this purpose since the carrier phase lock is a much more critical operation. Therefore, for the C/A-code synchronisation, the early and late magnitudes are computed from the related I and Q sums for every 1ms accumulation period. These sums are then averaged over the 8 milliseconds containing valid data in a 9 millisecond multiplexing period.

The initial state of the receiver is unlocked and the C/A-code synchronisation has to be obtained first. The hardware variable delay will therefore be scanned through all possible C/A-code phases (1023 for GPS and 511 for GLONASS) by incrementing the variable-delay counter in suitable steps (6 for GPS and 9 for GLONASS). When a signal magnitude above threshold is detected, the software switches to the synchronisation main-

taining routine. A suitable time-constant is built-in to prevent the loss of lock on short signal interruptions. In the synchronisation-tracking mode, the software performs as a second-order phase-locked-loop, computing the C/A-code phase and rate from the measured early-minus-late difference.

The signal carrier still includes the 50bps 0/180 BPSK navigation data, so a Costas-loop demodulator is required to obtain both the regenerated carrier for Doppler measurements and the 50bps navigation data. The Costas-loop demodulator operates on every 1ms signal sample I and Q components computed as an average on the early/late data. The loop feedback is a second-order network computing the carrier phase and frequency.

The carrier-lock operation is not simple. Initially, the whole frequency range from -500 Hz to +500 Hz is scanned. To prevent false locks, the scanning is stopped only when the residual loop error becomes small enough. Finally, the locking point needs to be checked for the +/-500 Hz ambiguity caused by the 1 kHz sampling rate. The latter ambiguity is resolved by counting the number of transitions in the demodulated data stream in every 8 milliseconds of valid data in a multiplexing period. Since valid GPS data only has transitions every 20ms (GLONASS every 10ms), there can be at most one transition in 8ms of data. If the frequency is wrong, there are at least six transitions and this can be detected easily.

Of course, the phase of both code and carrier PLLs need to be adjusted for the



following multiplex period, accounting for all of the time spent by the hardware processing the signals from the other satellites. In a navigation receiver the code phase and the carrier frequency are the main parameters to be measured, and these are supplied by the corresponding phased-locked loops. In addition to this, the code rate is also used by the software to compute a rough approximation for the carrier frequency and eliminate the ambiguity caused by the 1 kHz signal sampling rate. Before further processing, the code phase, code rate and carrier frequency are averaged over 16 multiplexing periods corresponding to a time span of 288ms (privileged satellite) or 864ms (other satellites). The averaged measurements are placed in a FIFO memory together with 1ms time tags to be read by the main program.

The last task performed by the interrupt routine is navigation data processing. The latter includes yet another PLL for bit synchronisation. This PLL locks on the transitions in the data stream. The demodulated 1ms samples containing the transitions are rejected, while all of the other available samples for a given satellite are accumulated into bits (GPS) or half-bits (the GLONASS Manchester phase is not known yet).

The following navigation data processing depends on the data format and this is slightly different between GPS and GLONASS. The GPS data is formatted into 30-bit words containing 24 true data bits and 6 parity-check bits. The word synchronisation is obtained by checking the parity bits, including the last two bits of the previous word, for

any possible word phase. The BPSK polarity ambiguity is also resolved by the parity bits. The synchronised and checked GPS data words are placed in another FIFO memory together with 1ms time tags, to be read by the main program.

The GLONASS data is formatted into lines with 85 data bits in Manchester format and a non-Manchester sync pattern, for a total duration corresponding to 100 bits. The sync pattern is not used in the GLONASS receiver in this project. The synchronisation is obtained by checking the 8 parity bits for any possible half-bit phase (200 possible phases), to resolve the Manchester phase ambiguity as well. Since the data bits are differentially encoded, there is no polarity ambiguity to be resolved. Like in the GPS receiver, the correctly received data lines are placed in another FIFO memory, together with 1ms time tags, to be read by the main program.

5.3 Main Program Loop Tasks

Since most of the functions performed by the main program loop require high-accuracy floating-point arithmetic, the main program is mainly written in the DSP computer high-level language. Of course, all of the interfaces to the interrupt routine and to the various peripherals (initialisation of the dedicated DSP hardware, LCD drive and the real-time clock chip) are at least partially written directly in the MC68010 machine code and are inserted in hexadecimal format in the main program source code.



The main program loop executes once for every new set of averaged measured data. The latter is available every 864 milliseconds for the three satellites that get less hardware time. The privileged channel supplies three separate sets of averaged data in the same time period, but the excess data is not used by the main program loop.

The main program loop also updates the LCD or writes a new line on a CRT display. The internal operation of the program is however independent of the selected menu on the display. The menu only affects the keyboard functions and some computations closely related to the format of the displayed data, like coordinate conversions.

The first task of the main program loop is to write the look-up tables in the dedicated DSP hardware memory. This operation is done at receiver power-up, when changing satellites, when adjusting the carrier frequency (in 1 kHz steps) or when switching the privileged satellite. The satellites can be selected manually, but usually the software is set to automatically select visible satellites.

When a given satellite is selected, the receiver requires some time to lock on its signal. The software will first look for all possible C/A-code phases. If the lock is not achieved, the main program loop will change the hardware look-up table frequency in 1 kHz steps in a given frequency range (20 kHz in the GPS receiver, or 25 kHz in the GLONASS receiver). Of course, the look-up table frequencies for all four satellites can also be preset manually.

The look-up tables are rewritten when switching the privileged satellite for several reasons. When all four satellites have been acquired this happens every minute, synchronised to the major data frames transmitted every 30 seconds from both GPS and GLONASS satellites. Since switching the privileged satellite includes some loss of data, other operations that corrupt the data, like rewriting the look-up tables, may be performed at the same time without any additional losses. The look-up tables are rewritten to correct for large variations in the Doppler shift or local reference oscillator drift. Further, the new look-up tables are rewritten with a randomly chosen phase relationship between the carrier phase and code phase, to avoid any possible interference between the carrier and the code when averaging the measured data over a longer period of time.

The main loop will then process all of the navigation data accumulated in the corresponding FIFO memory. The software looks for the frame sync and formats the data into frames. Additional checks are made before the formatted data is used. Correctly received frames are used to collect the precision ephemeris orbital data for the given satellite, to update this almanac containing less accurate data about the whole satellite navigation system and to set the GPS/GLONASS receiver real-time clock chip.

The next task is to collect the code phase and carrier frequency measurement results from the corresponding FIFO memory. The most recent data is always used together with the previous



sample to relate all of the data to a single time point using linear interpolation. This simplifies the following computations, since the positions and velocities of all four satellites need to be calculated for a single point in time.

The measured data and the satellite positions and velocities (computed from the precision ephemeris data) are then assembled into the navigation equations. A set of three time-difference navigation equations is obtained from code-phase differences and another set of three Doppler-difference navigation equations is obtained from carrier-frequency differences.

The time-difference navigation equations are solved first, using the Newtons method. The starting point is taken in the Earths centre ($x=y=z=0$). From this starting point the Newtons method requires between three and four iterations to converge to the final result for a user located on the Earths surface. The result in Cartesian coordinates x,y,z is then converted to longitude, latitude and height.

The position obtained may now be corrected for the propagation anomalies in the ionosphere and troposphere. The present software does not apply any correction for the ionosphere. The navigation equations are only corrected for the troposphere at the calculated height and the Newtons method is iterated once again to obtain the final result.

Since the position is already available from the time-difference navigation equations, the Doppler-difference navigation equations are solved to obtain the velocity of the user. Solving the Doppler-difference equations for the

velocity does not require a numerical iterative method, since the equations result linear for this unknown. The computed velocity vector is converted into magnitude, azimuth and elevation on the display.

The accuracy of the navigation solution depends on the geometry of the satellites. In place of the GDOP the software only computes the determinant of the linearised system of equations at the calculated position. This determinant is a dimensionless quantity. The higher the determinant, the more accurate the solution. If the determinant is too low, an error condition is signalled. The Doppler-difference equations have the same determinant if solved for velocity.

The main program loop also performs data averaging. Both position and velocity are averaged. Only good data with no error signalled is added to the average. The determinant of the system of equations is used as a weight for each new data set added to the average. Of course, the averaging buffer may be manually reset if desired.

The display includes several different menus and two of them are devoted to the immediate and averaged data. The position may be displayed in different formats: degrees only, degrees, minutes and seconds or Gauss-Krueger rectangular grid. Other menus are used to show the receiver status and the almanac data.

Finally, the main program loop usually also performs an automatic satellite selection. This function is triggered if an error condition is signalled continuously for a certain period of time (100 main loops). The software then uses the



almanac data and the real-time clock to find the visible satellites at the averaged user location. The receiver is then programmed for the four visible satellites with the highest elevations in the sky. Although this procedure does not yield the best GDOP its operation is foolproof.

5.4 Software Menus and Commands

Since a portable GPS/GLONASS receiver only has a small keyboard with a few keys and a small alphanumeric display, the various user commands need to be arranged into several different menus.

The keyboard has eight different keys, four of them (corresponding to ASCII characters 4, 5, 6 and 7) are used to select the four main menus. Depressing these keys only changes the content of the display and the functions of the other keys, but does not affect the internal operation of the GPS/GLO-NASS receiver. Some of these keys have additional functions if depressed more than once. Depressing key 4 cyclically shows all four virtual receiver channels (satellites) on the display. Depressing key 7 cyclically shows the general receiver status and the almanac data for all currently visible satellites.

The remaining keys (ASCII 0, 1, 2 and 3) are called parameter keys. Depressing these keys affects the internal operation of the GPS/GLONASS receiver as a function of the current menu. The mode of operation of these keys is also dependent on the actual

menu. Some functions allow a repeated action of these keys during just one main program loop (864ms), like setting the channel IF. Other functions are intentionally slowed down, like the total reset of the receiver. The latter requires depressing the corresponding key for at least 9 times and just one entry is allowed for each main program loop, to avoid unintentional loss of data.

In order to understand the commands of a GPS/GLONASS receiver it is necessary to understand the internal operation of the latter. A GPS/GLONASS receiver includes a non-volatile RAM to store the almanac data and a real-time clock that are always powered by a small internal NiCd battery. The non-volatile RAM is used to store the almanac data and the approximate user position as a result of a previous receiver operation. At power-up this data is used together with the real-time clock data to find all visible satellites and speed-up the acquisition of four usable satellite signals.

When a GPS or GLONASS receiver is first powered up, all of the non-volatile RAM contains random data and a total reset is required. The total reset erases all almanac data and puts the receiver in the manual satellite select mode. All receiver virtual channels are set to a central carrier frequency and a GPS PRN#16 or GLONASS CHN#13. The menu 4 is selected to show the virtual channel #1 data.

The initial satellite signal acquisition without any almanac data may take a large amount of time, especially in a single-channel receiver. The receiver



does not know which satellite to look for not its frequency offset caused by the Doppler shift and by the unknown frequency drift of the receiver itself. The current software for the GPS/GLONASS receiver in this project is not able to select different satellites automatically without any almanac data, so this has to be done manually.

After manually selecting the satellite(s), the software is going to try to achieve C/A-code lock. If the latter does not occur on the given IF frequency, the receiver is going to scan the expected IF frequency range in 1 kHz steps by writing the corresponding look-up table. Only the privileged satellite IF is scanned in the range from 2310 kHz to 2330 kHz (GPS) or from 1675 kHz to 1700 kHz (GLONASS).

While searching for the initial signal acquisition there is a small difference between the GPS and GLONASS receivers. The GPS constellation is now complete and more than four visible satellites can be found at any time, so the GPS receiver is only going to switch the privileged channel after a satellite signal is acquired. On the other hand, the GLONASS constellation is not complete and sometimes there is just one visible satellite, so the GLONASS receiver is going to try a different virtual channel with a different satellite if the current privileged satellite was not acquired.

After a satellite signal has been acquired, the key 4 menu shows the most important receiver parameters:

RX: virtual channel number
SV: GPS satellite PRN code number

CH#: GLONASS satellite RF channel number
CF: look-up table preset central IF frequency (kHz)
R: measured IF frequency (kHz, from code rate)
S: signal level (S-meter)
SVH: satellite health flag (0=OK)
URA: GPS user range accuracy (m)
ASF: GPS anti-spoofing flag (0=OFF)
En: GLONASS ephemeris upload age (days)
AOE: GLONASS ephemeris age (S)

If the receiver has been turned on for the first time, or has not been used for a considerable period of time (more than one week), the best thing to do is to collect the complete almanac data first. To speed-up the almanac data collection it is recommended that the remaining three receiver virtual channels are set to the same satellite and to the same IF frequency as the channel that already acquired a satellite. After all four virtual channels achieve data lock, the almanac data collection takes 12.5 minutes for GPS or 5 minutes for GLONASS, since the GLONASS receiver does not make use of half of the almanac frames.

The accumulated almanac data can be checked by repeatedly pressing key 7. The almanac data includes the satellite name/number plus the following information:

CH#: GLONASS RF channel number
EL: elevation (degrees)
AZ: azimuth (degrees)
DF: Doppler frequency shift (Hz, polarity as in the IF)



- A/E: GPS almanac/precision ephemeris data
- SVH: satellite almanac health flag
(GPS 0=OK;
GLONASS 1=OK)
- ASF: GPS anti-spoofing and configuration flag
- UTC: UTC date and time

The elevation, azimuth and Doppler shift are computed for the reference user position as obtained from the averaged data. After a total reset this reference position is set in central Europe. Checking the almanac it is possible to find out when the receiver can be switched to automatic satellite selection. In the automatic satellite selection mode, the program selects the four satellites with the highest elevations and sets the corresponding central IF values in the hardware look-up tables. This selection can be done immediately by pressing key 0 in menu 7, or by switching the program to do this automatically after a period of bad data (key 3 in menu 7).

After four satellites have been acquired the display may be switched to menu 5 or 6 to show respectively the immediate or averaged data.

These menus show the following:

- DET: determinant of the system of equations (menu 5 only)
- AVG: averaging weight (menu 6 only)
- V: velocity vector magnitude (km/h), azimuth and elevation
- LAT: latitude (degrees or n, north)
- LON: longitude (degrees or m, east)
- H: height above ellipsoid (m)

At the beginning of all menus (except the almanac) the receiver status error codes appear. These codes show the general receiver status, the current privileged virtual channel and the status of the single virtual channels. Most of the codes used are obvious, but three of them require further explanation. In the general receiver status code P means that the computed position deviates too much from the previous main program loop. On the other hand, code E is only activated after the averaging weight gets larger than 5, and means that the equations themselves deviate too much from the already computed average position. Finally, code T in the virtual channel status appears quite frequently since the current software does not handle the overflow of the C/A-code variable-delay counter correctly.

Finally, the general status menu (key 7) shows some interesting data about the receiver; the satellites currently selected, AUTOMATIC or MANUAL satellite selection, the measured nominal IF frequency of the receiver (without the Doppler shift), the measured receiver master oscillator frequency and the UTC date and time.

6. CONCLUSION

The GPS and GLONASS systems are mainly intended for navigation, but there are many other less advertised but not less important, not less interesting applications of these systems. Since



these systems are known and the technology to use them is available to anyone, we radio amateurs should consider our own applications of these systems [13].

Although the navigation itself is not of much interest to radio amateurs, it would probably make more sense to transmit GPS or GLONASS coordinates of a contest location, rather than the inaccurate EU or WW locator, which is already not accurate enough for serious microwave or laser communications. By the way, GPS and GLONASS use almost the same coordinate system and a long time average shows differences of the order of only 10m between the systems.

A side product of both GPS and GLONASS is accurate time and frequency broadcast. In order to achieve the specified navigation accuracy the timing measurements have to be performed to an accuracy of about 10ns. The same requirement applies to the on-board satellite atomic clocks. The final user time transfer accuracy ranges between 30ns and 100ns, depending also on the knowledge of the exact user location. Thus the user should also compute his position even if he only needs accurate time

Radio amateurs could use this time transfer capability of both GPS and GLONASS every time when accurate synchronisation is required. Coherent communications are just an example, the accuracy of GPS or GLONASS offers more than this. For example, the actual propagation path of the radio signal and the propagation mechanism could be investigated in this way.

The frequency broadcast accuracy of both GPS and GLONASS is in the range of 10-12, far better than can be achieved with HF or LF standard frequency transmitters. The accuracy of the latter is limited to around 10⁻⁷ by the propagation effects alone, and this is not enough for serious microwave work. GPS and GLONASS are also available globally 24 hours per day and are not limited by the transmitter range.

Finally, GPS and GLONASS represent a step away from being just an operator of black-box amateur radio equipment. Although there are several ready-made GPS receivers on the market we will probably have to develop our own receivers for our experiments, both the hardware and the software. Building such a receiver may be an interesting challenge as well. The receiver shown in this article is perhaps just the first step, other related projects or better receivers will follow soon.

This completes this construction project, although the editor feels certain that further articles on the subject in general and this project in particular may appear in future issues.

A complete list of all literature references follows on the next page.

A complete list of kits and printed circuit boards for this project appears on page-255 of this issue.



7.

REFERENCES

- [1] Matjaz Vidmar: "Digital Signal Processing Techniques for Radio Amateurs, Part-2: Design of a DSP Computer for Radio Amateur Applications"; VHF Communications 1/91, pp 2-24
- [2] Matjaz Vidmar: "Digital Signal Processing Techniques for Radio Amateurs, Part-3: Construction and use of the DSP Computer"; VHF Communications 2/89, pp 74-94
- [3] Jonathan S. Abel, James W. Chaffee: "Existence and Uniqueness of GPS Solutions"; pages 952-956/6-91, Vol.27 IEEE Trans. on Aerospace and Electronic Systems
- [4] "Interface Control Document MHO8-00002-400, rev-E", (84 pages), August 7th, 1975, Rockwell International Corporation, Space Division, 12214 Lakewood Boulevard, Downey, California 90241, USA
- [5] "Interface Control Document GPS-200", (102 pages), August 7th, 1975, Rockwell International Corporation, Space Operations and Satellite Systems Division, 12214 Lakewood Boulevard, Downey, California 90241, USA
- [6] "Global Satellite Navigation System GLONASS Interface Control Document" (46 pages), 1988, Research-and-Production Association of Applied mechanics. Institute of Space Device Engineering, Glavkosmos, Russia
- [7] Robert C. Dixon: "Spread Spectrum Systems", (422 pages), 1984, Second Edition, John Wiley & Sons, New York, USA
- [8] Matjaz Vidmar: "Digital Signal Processing Techniques for Radio Amateurs, Theoretical Part"; VHF Communications 2/88 pp 76-97
- [9] P. Mattos: "Global Positioning by Satellite", (16 pages), Inmos, Technical note 65, July 1989
- [10] J. B. Thomas: "Functional Description of Signal Processing in the Rogue GPS Receiver", (49 pages), June 1, 1988, Jet Propulsion Laboratory, California Institute of Technology, Pasadena, California, USA
- [11] Charles C. Kilgus: "Shaped Conical Radiation Pattern of the Backfire Quadrifilar Helix", (pages 392-397), IEEE Transactions on Antennas and Propagation, May 75
- [12] Matjaz Vidmar: "A Very Low Noise Amplifier for the L-Band"; VHF Communications 2/92 pp 90-96
- [13] Matjaz Vidmar: "Radio Amateur Applications of GPS/GLONASS Satellites: Using GPS/GLONASS Satellites as an Accurate Frequency/Time Standard"; (pages 186-190), Scriptum der Vortraege, 37 Weinheimer UKW Tagung, 19/20 September 1992

Dipl. -Ing. Detlef Burchard, Box 14426, Nairobi, Kenya

Linear Signal Rectification

Part-2 (conclusion)

As was demonstrated in Part I, it is scarcely possible to obtain anything better than 1% accuracy using semiconductor diodes and passive components. It is necessary to use amplifiers for more precise conversion. The expression "active rectifier" has gained currency in this connection.

In principle it would be possible to amplify the signal voltage to several hundred Volts in order to get some way below the 1% hurdle. Or else to equalise the quadratic range using a non-linear secondary amplifier, as described in Burchard [1]. However, this is not what is understood by the term "active rectifier" in present usage. The diodes have to be mounted in the feedback loop of an amplifier for it to become an active rectifier! The overall characteristics are thus dependent on the properties of the amplifier.

1. INTRODUCTION

Any book which deals with applications for operational amplifiers also discusses rectifier circuits. Now, a rectifier always has an AC value (voltage or current) as the input value; an amplifier which operates right down to DC current is really not at all necessary. In fact, active rectifiers had already been developed before there were any opamps (operational amplifiers). In some ways, they provided better data than can be obtained using opamps. With opamps you can construct rectifiers which have no diodes and, instead of diodes, better transistors can be used in other circuits. All of this should be understood here as covered by active rectifiers. These selected examples can

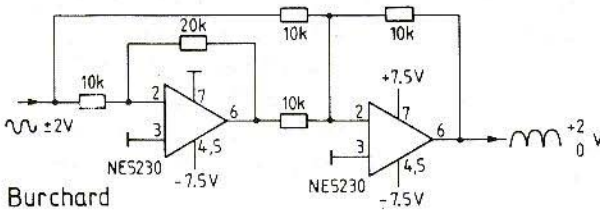


Fig.1:
Rectifier Circuit
"without rectifiers"



make no claim to providing an exhaustive list. However, there are circuits which have been tried and tested in practise and work more accurately than simple diode circuits.

2. THE CIRCUIT WITHOUT DIODES

There are opamps which can amplify only voltages of one polarity. These are the types with input and output voltage ranges which include one of the operating voltages, which is then selected as zero. Fig.1 shows a suitable circuit. The first opamp is only supplied by one negative operating voltage. Its output can accept only negative values. It thus amplifies only the positive half-waves of the input voltage, by a factor of two. The negative unamplified voltage is added to the doubled positive voltage in the second opamp to give two-way rectification. The first amplifier must fulfil specific conditions: to be latch-up free and to have low offset voltages in the vicinity of the positive operational voltage. An amplifier without these special characteristics requires 1 or 2 diodes in the circuitry to give the same result. Nevertheless, the circuit does have a disadvantage: one half-wave passes through an additional amplifier and is thus dependent on the characteristics of this amplifier, which has phase and amplitude errors at high frequencies. The circuit in Fig.1 is thus suitable only for the low-frequency range and does not reach the 0.1% error

limit, due to the offset voltage. In principle, we are dealing with momentary value rectification, which can be changed into mean value rectification by integration in the second amplifier. The circuit, which was taken from [4], may not have a capacitor at the input to isolate the DC voltage because the input resistance is not constant due to the non-linear mode of operation of the first opamp. Should one nevertheless be included, an additional opamp is necessary to act as a buffer stage.

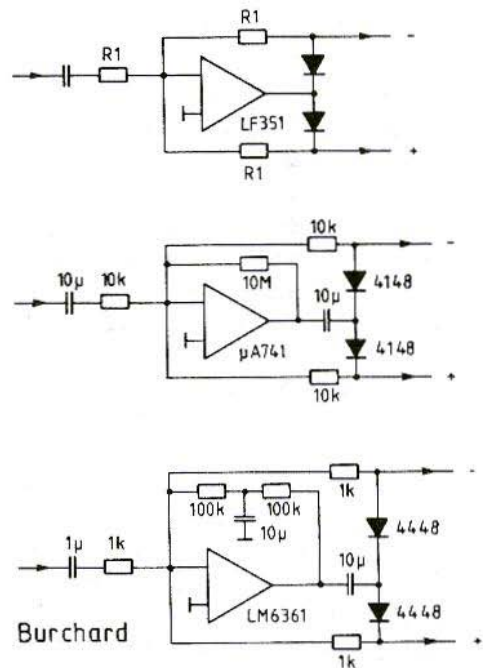


Fig.2: Separation of Positive and Negative Half-Waves using an Operational Amplifier

- a) generally, when amplifier bias current is negligible
- b) with low bias current
- c) with high bias current

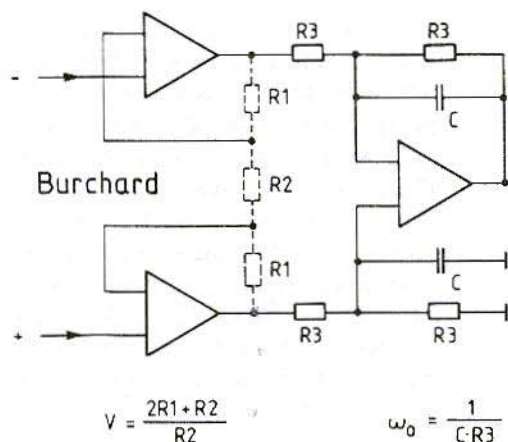


Fig.3:
Instrumentation Amplifier
made from three Opamps,
and Dimensioning Formulae
Components R1 and R2 are
required if Amplification
desired exceeds 1

3. CONSIDERATION OF FREQUENCY RESPONSE

Normal resistance levels in operation amplifier circuits are approximately $10\text{k}\Omega$. This value is suitable for normal output loads of $2\text{k}\Omega$. The output division may be up to 5. We are dealing here with diode capacities of from 1 to 4pF , which means $Z = 10\text{k}\Omega$ between 4 and 16 MHz. 0.1% error values are thus already being attained between 40 and 160 kHz. If we want to work with a considerably higher frequency range, the computing resistances should be considerably lower. In order to remain stable with any feedback, opamps have a steadily falling frequency response; amplification $v = 1$ is attained between 0.5 and 50 MHz. A significant improvement, as against a passive rectifier, also requires significant reserve amplification which, if it has to be, for example, 100, can mean only that active rectifiers can work, at best, with opamps in the range between 5 and 500

kHz. The increase in precision is purchased at the cost of a reduction in the band width. Circuits with opamps, even with extremely rapid types, can thus in general be used only in the audio frequency range or just above it.

4. OPERATIONAL AMPLIFIER CIRCUITS

The disadvantage in the circuit from Fig.1 can be avoided in the opamp if both half-waves are amplified. Two diodes are now required to isolate the half-waves, as in Fig.2a. The circuit has two outputs, which are actually separated into positive and negative half-waves, which is sometimes desired for separate processing. However, as a rule the difference between the two outputs is desired, and an instrumentation amplifier is added which is bought ready-made as an integrated circuit, or which

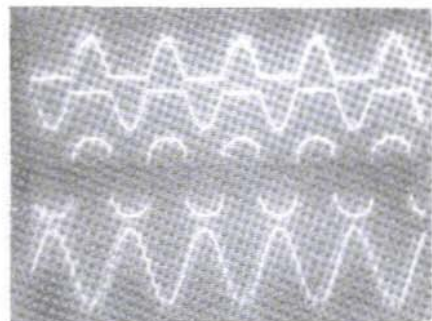
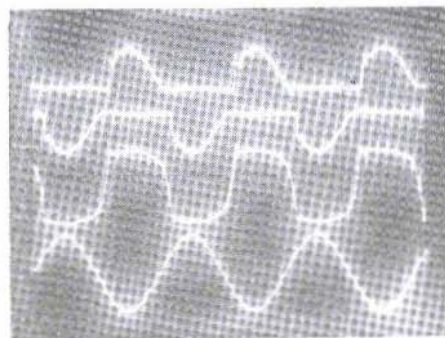


Fig.4:
Nearly Ideal Half-Wave Separation
for low Frequencies (here 100 Hz)
and Adequate Amplification Reserve
(LF 351 Opamp)

Y1: + Output 50 mV/div
 Y2: - Output 50 mV/div
 Y3: Opamp Output 500 mV/div
 Y4: Input Signal 50 mV/div
 X: 5 ms/div

you can build yourself, as per Fig.3, from three opamps (a dimensioned example with CMRR and zero point trimming can be found below in Fig.9). The capacitors, C, give a mean value measurement from the original momentary value.

The input current from the opamp may lie several orders of magnitude above the reverse current of the diodes, causing the circuit - Fig.2a - to become asymmetrical. A way out is to separate the AC and DC paths in the feedback consequently. An opamp with a relatively low input current (example UA 741) can be wired up like Fig.2b, while one with a relatively high input current needs a circuit like Fig.2c; this, then, is suitable, for example, for an LM 6361.



In the latter case, the computing resistances are selected to be lower and low-Ohm diodes used to make correct use of the faster opamp. It is in no way the case, as you may sometimes read, that there is no feedback without an input signal. Two Si-diodes or Schottky diodes, according to Burchard [1], have R_0 at 50 or 1.5 $M\Omega$. The initial amplification is thus set at 5,000 or 150, and lies considerably below the open-loop voltage gain of opamps at low frequencies. A low R_0 is also the reason why Ge diodes and opamps together do not produce a better rectifier. The computing resistances would have to be set so low that most opamps could no longer drive them. The forward voltage of the diode is rendered harmless by the opamp - the more so,

Fig.5:
Inadequate Half-Wave Separation at
high Frequencies (here 300 kHz) and
inadequate Amplification Reserve
(LM 6361 Opamp).

Calibration as in Fig.4, but X: $\mu s/div$

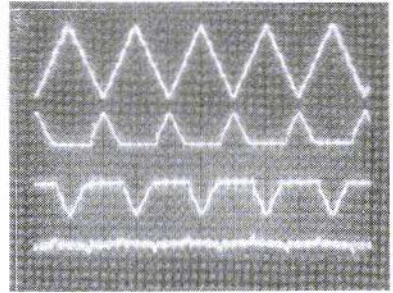
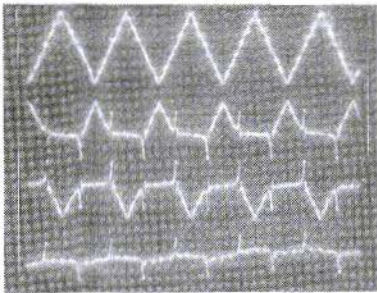


Fig.6: App. 10% Error in Half-Wave Area leads to the Conclusion that the Rectifier is still processing 10 times the Frequency, or 1/10 of the Voltage, even if with an Error of up to 100%

- a. LM 6361 Opamp, 100 kHz b. 741 Opamp, 1 kHz

Y1:	Input Signal 50 mV/div	5 mV/div
Y2:	+ Output 50 mV/div	5 mV/div
Y3:	- Output 50 mV/div	5 mV/div
Y4:	Error Voltage at Inverting Opamp Input	
	50 mV/div	5 mV/div
X:	5 μs/div	500 μs/div

the higher the residual amplification is. At low frequencies, the oscilloscope gives us an image like the one in Fig.4 - beam trace 3. The output changes polarity so fast that no trace comes appears. As desired, the two outputs provide the separated half-waves without any visible errors.

This clearly ideal behaviour changes if

the opamp no longer has sufficient open-loop voltage gain. This is the case with standard opamps, even at amazingly low frequencies. An LM 6361 with an gain-1 frequency of 50 MHz, however a low amplification of 400, which therefore remains rather constant up to about 100 kHz is already over-stretched at 300 kHz (Fig.5). The

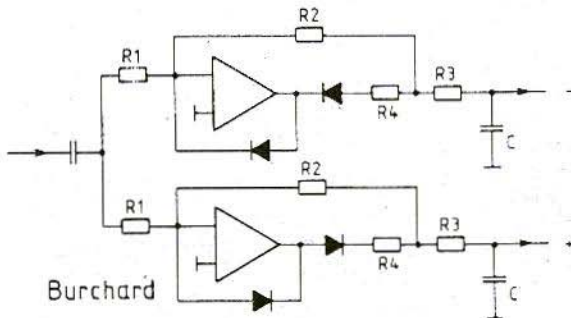


Fig.7: General Circuit for the four Types of Evaluation



WEIGHTING	R1	R2	R3	R4	C
Mean Value	22k	24k	0	0	0
Quasi-Effective Value	43k	24k	6k2	0	10 μ F
Quasi-Peak Value	680k	240k	1k	0	1 μ F
Peak Value	680k	240k	0	100	10 μ F

Table 1: Dimensioning of Circuit in Fig.7, approximate Scaling for Display of Effective Value with Sinusoidal Form

output voltage can no longer change rapidly enough. Fractions are missing in the half-waves of the separated outputs. If we estimate them at 20%, then it would still be possible to measure the frequency referred to with a measurement range of 10 Vpp with an error of only 0.2%. Lower frequencies can naturally be measured more precisely, and a small improvement can also be obtained at all frequencies if the diodes are biased with more than 300mV.

Fig.6 shows another kind of error detection. The voltage at the (-) input of the opamp corresponds to the conversion error, namely the difference between input and output voltage. If this fraction is small (app. 10% in each case in the diagram sections), then the conversion is correspondingly precise. Diagram section Fig.6a shows therefore how a 100 mVpp signal of 100 kHz

allows the conclusion to be drawn that a measurement range of 10 Vpp can go up to 100 kHz with a 0.1% error. Diagram section Fig.6b, with a 1 kHz signal of 10 mVpp, lets us conclude that a measurement range of 10 Vpp and a 0.1% error at up to 10 kHz would be attained.

5. FOUR TYPES OF EVALUATION

Diode rectifiers could be designed as per [1], to evaluate the mean, quasi-effective, quasi-peak or peak values. That is initially not possible with the active rectifiers from Figs. 1 and 2. They evaluate the momentary value and, following smoothing using a low-

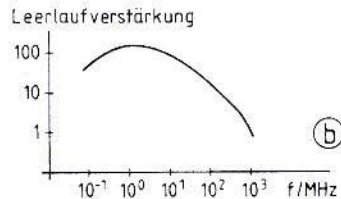
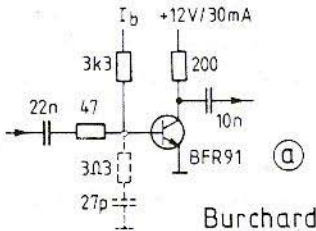
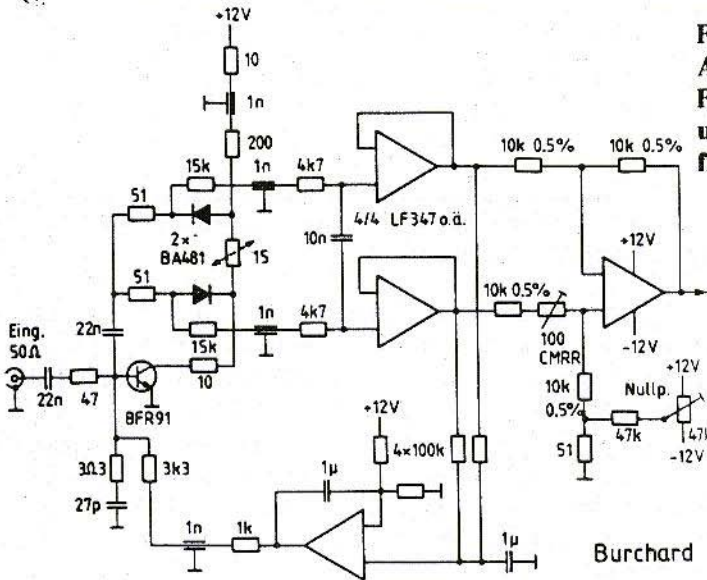


Fig.8: High-Frequency Operational Amplifier with Transistor (a) and its Bode Plot (b)

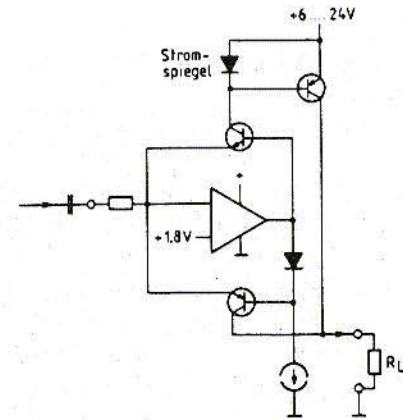
Leerlaufverstärkung = Open-loop Voltage Gain

Fig.9:
Active High-Frequency Rectifier using Amplifier from Fig.8



Burchard

pass, the mean value. Fig.7 shows a general circuit which takes all four weightings into account. The resistances, R_4 , are required if $R_3 = 0$ and $C > 0$. R_2 determines the discharge time, R_3 the charging time, for half-wave circuit. Again, an instrumentation amplifier is connected to the outputs. Table 1 gives the dimensions for the 4 types of evaluation. If the circuit is constructed using FET opamps, which have an f_l of app. 5 MHz, it will operate satisfactorily over the entire low-frequency range up to 20 kHz. The instrumentation amplifier to be added subsequently can also be fitted with FET opamps at the input, so that the load on the charging capacitors disappears. The entire universal rectifier is



Burchard

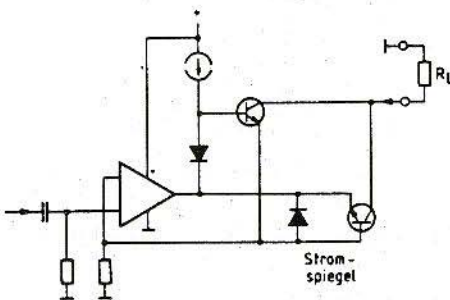


Fig.10:
Principle of Use of Transistors as Rectifiers

- a. In Comander IC NE 570
 - b. In Circuit of Fig.12
- Stromspiegel* = Current Mirror



Burchard

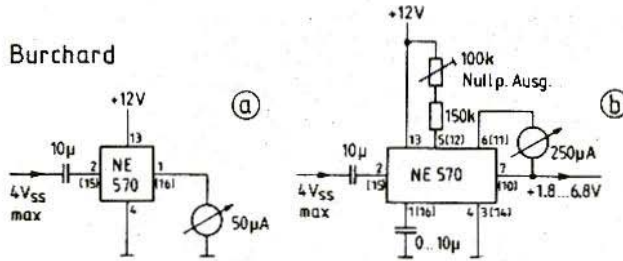


Fig.11:
Wiring of an NE 570 as
a Rectifier (a) and Use
of Internal Amplifier (b)
Nullp. Ausg. = Zero
Point Output

then to be put into effect with one LF 347 and one UA 741. The latter takes over the function of the opamp shown on the extreme right in Fig.3. The capacitors connected up here take over the formation of the mean value, or permit a wider reduction of the residual ripple. This is important for obtaining a steady display with subsequent A/D conversion and digital display.

6. HF OPERATIONAL AMPLIFIER

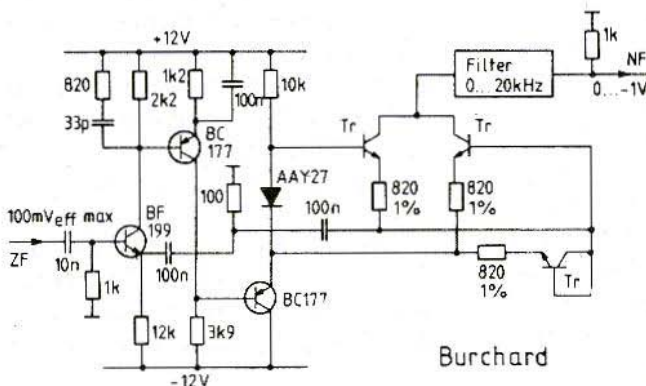
An individual high-frequency transistor in a circuit in accordance with Fig.8a forms an operational amplifier which certainly has a low open-loop voltage

gain, low input resistance and high output resistance, but which in addition has a remarkable fl frequency greater than 1 GHz. The RC combination shown dotted at the base gives this opamp a smooth frequency roll-off, which will now allow any feedback.

The Bode frequency response is shown in Fig.8b and from it we can see that between 0.1 and 30 MHz a rectifier can be expected to improve by a factor of more than 30; the linear range, which otherwise begins at 2 UT, can be expanded downwards to a few mV.

Fig.9 shows a suitable circuit, where we now also have a fully dimensioned instrumental amplifier. The fourth amplifier in the LF 347 is used to set the operating point of the BFR 91.

Schottky diodes are used as rectifiers and, together with the low load



Burchard

Fig.12:
Circuit of an Active
AM Demodulator in a
Modulation
Measurement Device

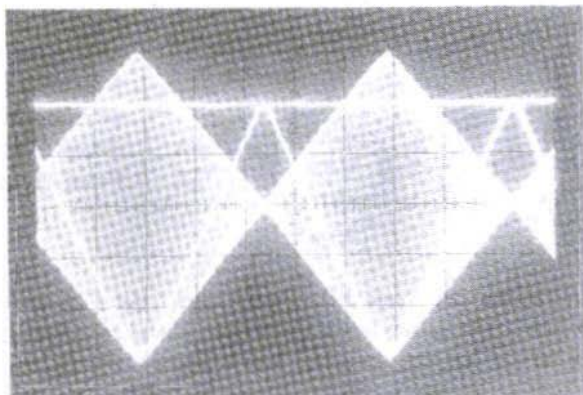


Fig.13: Demodulation of 100% Modulation by means of Circuit from Fig.12
Y1: 11 MHz Carrier modulates at 1,000 Hz, 10 mV/div
Y2: Demodulator Output with superimposed Zero Line, 200 mV/div
X: 200 μ s/div

resistors, allow momentary value rectification at up to approximately 50 MHz. The subsequent RC filter makes it possible to obtain a mean value. The Schottky diodes need a bias voltage to operate optimally. It is obtained from a 15Ω resistance and provides for a bias current of app. $10\ \mu\text{A}$.

Even better would be a bias voltage with a T of $-4\ \text{mV/K}$; then the bias current would be independent of the temperature. Unfortunately, there are no components with this characteristic - however, using an NTC would help. The portion of the circuit to the left of the feedthrough capacitors must be structured for the RF point of view - the more compactly, the better. If this is wired up to have a very low capacitance and inductance, the rectifier can make very accurate measurements between 0.1 and 100 MHz, and from 2 to 500 mV. The input has an impedance of app. 50Ω and is thus

suitable for standard high-frequency systems.

7. TRANSISTORS AS RECTIFIERS

The use of transistors instead of diodes has the advantage that the control current at the base amounts to only a small fragment of the emitter current. The majority of the emitter current leaves the component as collector current and can be referred to a completely different voltage level. If current mirrors are used simultaneously, simple circuits are obtained for a full-wave rectifier. Fig.10 shows two of these. You can buy such a circuit in integrated form such as the Compander IC NE 570. It is characterised by the

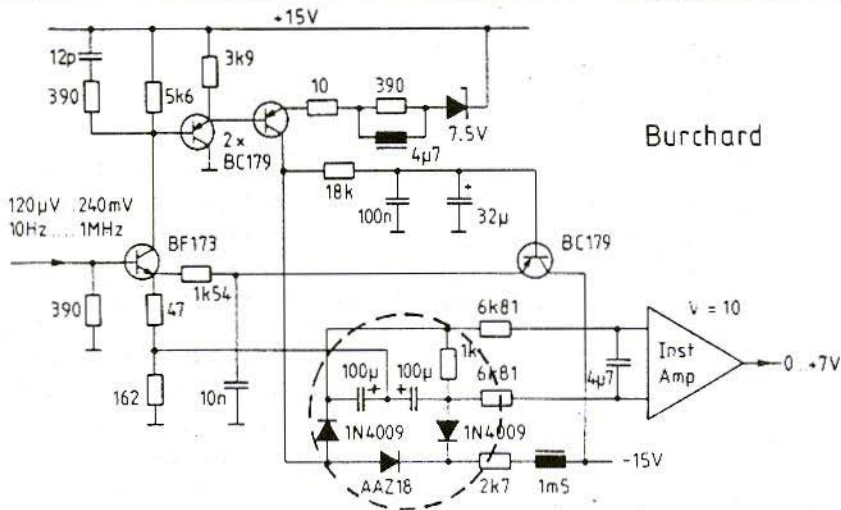


Fig.14: Rectifier (AC/DC Converter) for a 3½ Digit Multi-Meter

symmetrical structure of the rectifier, with complementary transistors around an opamp. The positive half-wave is reflected on the positive supply voltage and then added to the negative. The current output drives RL. Each IC contains two such rectifiers, which are to be connected up as per Fig.11a. For more information, see data sheet [3] from the manufacturers.

The IC also includes an opamp, with which the rectifier current can be amplified. Fig.11b shows the circuit for this. A capacitor can now also be provided at pin-1 (16), which causes the momentary value to create a mean reading. According to the manufacturer, the IC can be used in the audio frequency range with an error of app. 0.5%.

I myself designed the other circuit in Fig.10b 25 years ago for a modulation meter. In that context, it acts as an AM demodulator on the last intermediate frequency, between 400 and 600 kHz.

Instead of an opamp, transistors are used in an AC amplifier. Only NPN types are needed for the rectification, because a current mirror has been mounted directly in the counter-coupling.

The circuit is shown in Fig.12 with its final dimensions. High-frequency transistors with largely identical on-state characteristics are used for the transistors - marked as TR - so they should be either in a transistor array or carefully matched.

The outstanding characteristics of the circuit are illustrated in the oscillogram in Fig.13. The demodulation of a 100% modulated high-frequency signal shows no visible error.

The filter at the output of this demodulator is an LC filter with 2% ripple, which is characterised by the fact that it operates without a termination at the left-hand port. The entire output current thus flows through the 1kΩ termination

at the right-hand port. The above circuit uses no integrated components of any sort and can thus be designed rapidly enough by a skilful developer for use in the medium-wave frequency range.

Silicon diodes can also be used in the rectifier, as the last example shows. It also dates from a time in which opamp IC's were decidedly reasonable (less than DM 50 for a UA 709).

8. "ANTIQUÉ" PRECISION RECTIFIER

The circuit originates from the PM 2421 digital multi-meter [2]. It represents a mean value rectifier for the remarkable frequency range from 10 Hz to 1 MHz and has no conversion errors greater than 120 μ V (0.05%, referred to the input).

The transistor on the far right deals with the operational point stabilising. The others provide sufficient amplification for strong feedback over the broad frequency range.

In this equipment, the instrumentation amplifier is a super emitter follower with a double transistor, which is followed by a UA 709.

The specifications obtained are so good that, even 25 years later, it is not easy to repeat them, especially if you are ambitious enough to do without discrete components.

9. CONCLUSION

Active rectifiers operate as rectifiers with normal Si or Schottky diodes, or also with transistors, and amplifiers with single-sided cut-off. The circuits can take an enormous number of forms, of which only a very small selection could be shown here. It is relatively easy to obtain a precision of better than 0.1%, but only for a restricted frequency range. If opamp IC's are used, this does not exceed the audio frequency range significantly. Using lumped elements can take things somewhat further and finally an individual transistor can prove to be superior if you wish to operate in the 100 MHz range.

10. LITERATURE

- [1] D.Burchard (1994): Linear Signal Rectification - Part 1
VHF Communications 3/95,
pp. 168-179
- [2] N.N. (1969): PM 2421 DMM
Handbook: Philips Industrie-
Elektronik, Hamburg
- [3] N.N. (1986): Product Specification
NE 570/571/SA 571: Linear
Products Data Handbook IC
11, Philips, NL-Eindhoven
- [4] N.N. (1986): Product Specification
NE/SA 5230: Linear Products
Data Handbook IC 11, Philips,
NL-Eindhoven



Harald Fleckner, DC8UG

A 10 Watt Power Amplifier for the 13cm Band using GaAs Technology

Developed with the help of PUFF CAD Software

The two-stage power amplifier introduced in issue 3/1994 [1] of VHF Communications supplies an output power of 5 Watts in the 13cm band in linear operation (class A) with 23 dB amplification.

The article below introduces a new amplifier in this development range, which yields an output power of 10 Watts with a linear amplification of 20 dB.

The circuit and layout have once again been set up using Puff CAD software [4], on the basis of the results from the development work on the 5 Watt amplifier. As a result of this, a parallel circuit with two 5 Watt stages has been inserted in the high-level stage of this amplifier unit.

1. CHOICE OF SEMICONDUCTOR

The transistors used in the amplifier are Mitsubishi GaAsFETs from the 0900 range. The 0905 type is used in the driver stage, with two type 0906's in the parallel high-level stage.

The following performance data were the targets aimed for in the development work:

Amplification:	> 20 dB at K > 1
Output power:	Min. 10 W at max. 1 dB compression
Band width:	100 MHz
Zin = Zout:	= 50Ω with return loss > = 20 dB

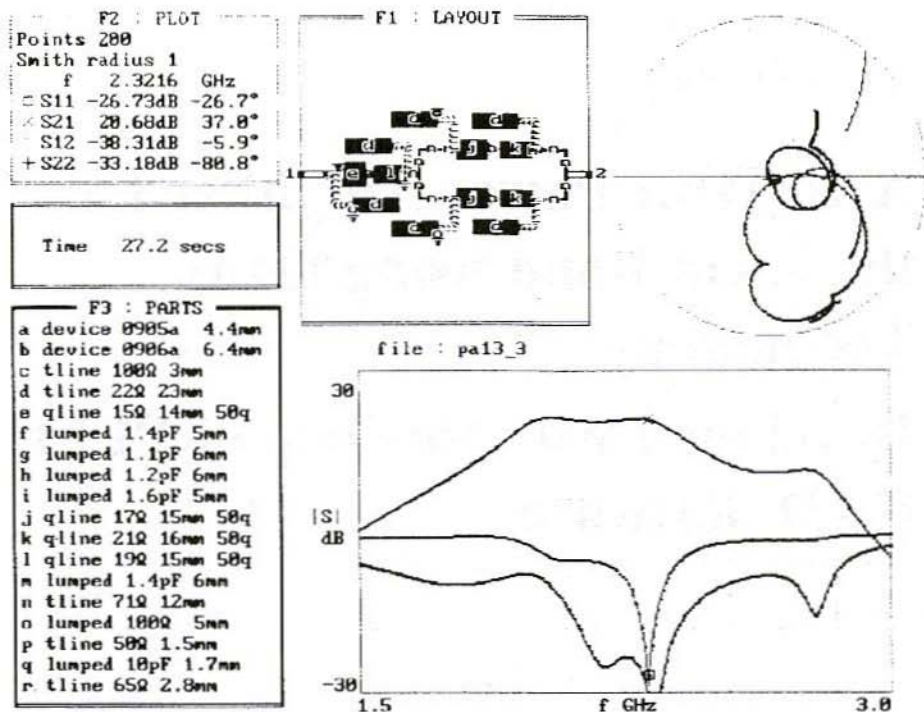


Fig.1: PUFF CAD Program Screen Print-Out

Arguments in favour of using a parallel high-level stage consisting of two 5 Watt transistors (as opposed to a single stage with a 10 Watt transistor) are the higher efficiency and the higher (in total) power loss of the parallel-switched high-level stage transistors and the, at present, rather more favourable cost/performance ratio of the 0906 GaAsFET, as against the 10 Watt 0907 type.

According to the Mitsubishi data sheet, in the given frequency range the 0906 attains an output power of 5.0 Watts = 37 dBm at $U_{ds} = 10$ V, $I_{ds} = 1.1$ A, with an amplification of 11 dB at 40% efficiency.

In comparison with the 0907 type (40 dBm output power / 10 dB / 37%), there is a lower power advantage in favour of the two parallel-wired 0906 stages.

The 0905 type comfortably supplies the necessary drive power of app. 1 Watt for the parallel stage with an amplification of approximately 10 dB. Its typical power is given by Mitsubishi as app. 34 dBm = 2.5 Watts at 8 V / 0.8 A.

The S-parameters for the selected transistors required for the circuit development are taken from the Mitsubishi data bank and are valid for the DC voltage conditions referred to above.

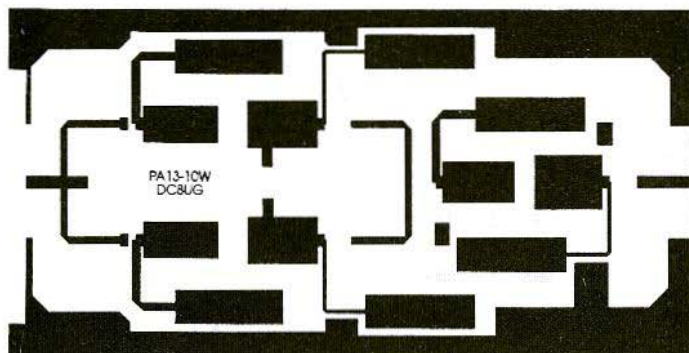


Fig.2:
PCB Layout for the
10 Watt High-Level
Stage

In operation, there is a DC input power exceeding 30 Watts, so the heat sink must have generous dimensions, in order to guarantee that the maximum permissible temperature for the transistors, of 175° is never reached.

2. SIMULATION AND ANALYSIS OF AMPLIFIER CIRCUIT USING CAD SOFTWARE

The functioning of the Puff CAD software is comprehensively described in [2] [3] [4], so only the results obtained are presented and analysed here. Fig.1 shows the screen print-out from Puff with the draft layout of the circuit, the associated Smith diagram, the parts list and the scatter parameter curve over the selected frequency range (1.5 - 3.0 GHz).

From the calculated scatter parameters, the stability factor, K, of the amplifier circuit can be subsequently determined for the operating frequency (2.3216 GHz) [5]. When plotted against the

frequency, the gain slope obtained (S21) clearly shows the influence of the 71Ω $L/4$ coupler between the two high-level transistors. This type of coupling pre-supposes a transformation of all individual stages with a 50Ω impedance, and is well known from aerial engineering. It is relatively loss-free and is particularly effective when each individual stage is transformed before the hook-up on the calculator to $Z_{in} = Z_{out} = 50\Omega$. The better this transformation is carried out, the "smoother" the gain slope actually obtained is, plotted against the frequency.

The calculated input impedance (S11) is more strongly dependent on the frequency than the output impedance (S22), and here the typical broad-bandedness of parallel stages shows to advantage. The values shown in Fig.1 give the following performance values for the simulated circuit at an operating frequency of 2,320 MHz:

Return loss input:	- 26.7 dB
Return loss output:	- 33.2 dB
Amplification:	+ 20.7 dB
Feedback:	- 38.3 dB
K factor at 2,320 MHz:	29
Power band width (-3 db):	- 400 MHz + 100 MHz

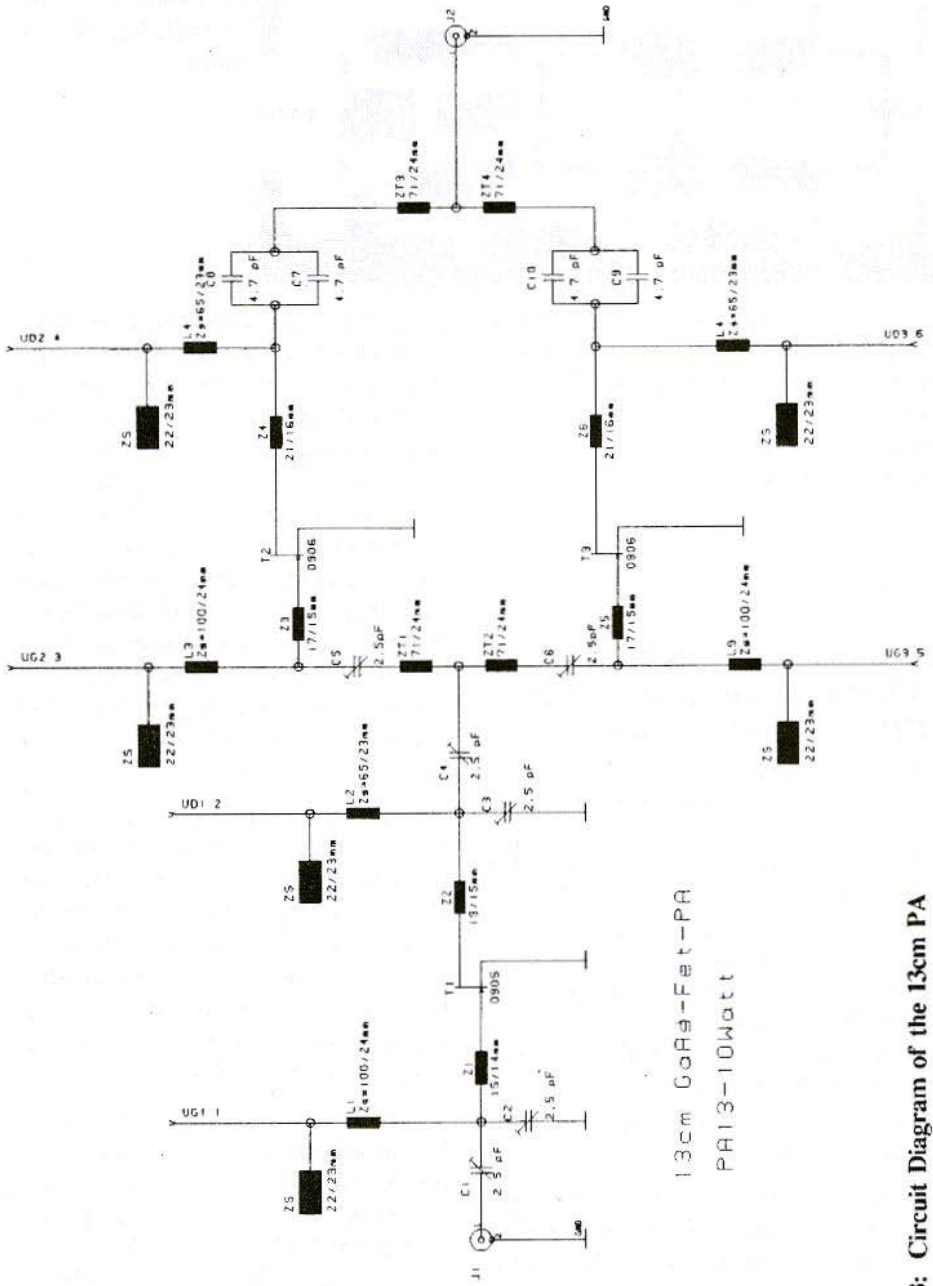


Fig.3: Circuit Diagram of the 13cm PA



C1	Trimmer	2.5pF	Teflon/Ceramic
C2	Trimmer	2.5pF	Teflon/Ceramic
C3	Trimmer	2.5pF	Teflon/Ceramic
C4	Trimmer	2.5pF	Teflon/Ceramic
C5	Trimmer	2.5pF	Teflon/Ceramic
C6	Trimmer	2.5pF	Teflon/Ceramic
C7	Capacitor	4.7pF	ATC-Chip 100
C8	Capacitor	4.7pF	ATC-Chip 100
C9	Capacitor	4.7pF	ATC-Chip 100
C10	Capacitor	4.7pF	ATC-Chip 100
J1	Socket	N-type or SMA	
J2	Socket	N-type or SMA	
L1	Inductor	100/24mm Stripline	
L2	Inductor	65/23mm Stripline	
L3	Inductor	100/24mm Stripline	
L4	Inductor	65/23mm Stripline	
L5	Inductor	100/24mm Stripline	
L6	Inductor	65/23mm Stripline	
T1	FET	0905	Mitsubishi
T2	FET	0906	Mitsubishi
T3	FET	0906	Mitsubishi
ZS	Inductor	22/23mm Stripline	
Z1	Inductor	15/14mm Stripline	
Z2	Inductor	19/15mm Stripline	
Z3	Inductor	17/15mm Stripline	
Z4	Inductor	21/16mm Stripline	
Z5	Inductor	17/15mm Stripline	
Z6	Inductor	21/16mm Stripline	
ZT1-ZT4	Inductor	71/24mm Stripline	

Fig.4: Parts List for the 13cm 10W PA

Fig.2 shows the layout generated by the CAD software as a laser print-out, for Teflon-based material with a substrate thickness of 0.79 mm..

The earth paths on the longitudinal and transverse sides of the boards are surfaces which are added later and which are through-hole plated to the underside of the boards.

In the parts list in Fig.1, we can also

recognise the necessary discrete components of the circuit, under the description "lumped". Here we are dealing with capacitors and resistances which are necessary for the circuit to operate.

Fig.3 shows the wiring diagram for the 10 Watt parallel high-level stage. Fig.4 shows all components required in the parts list.

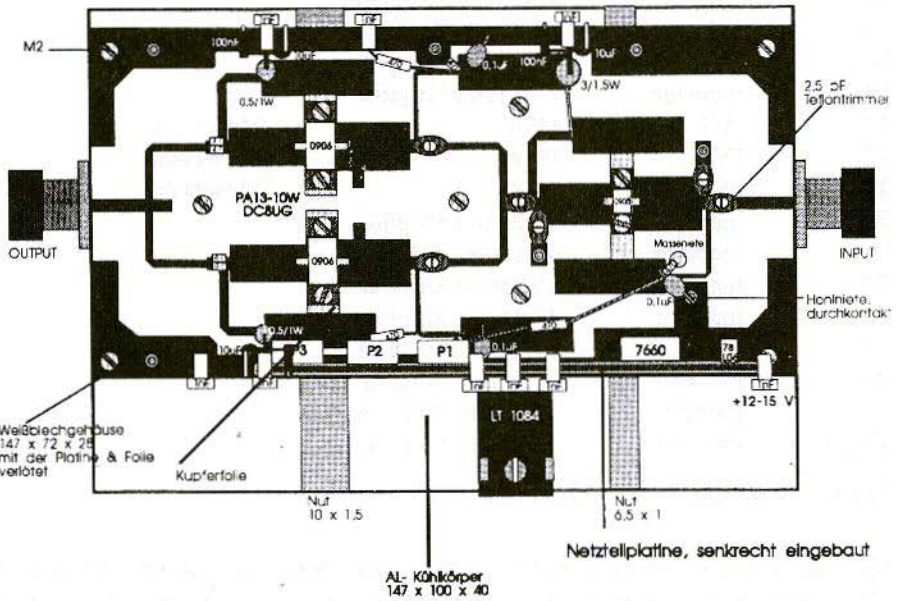
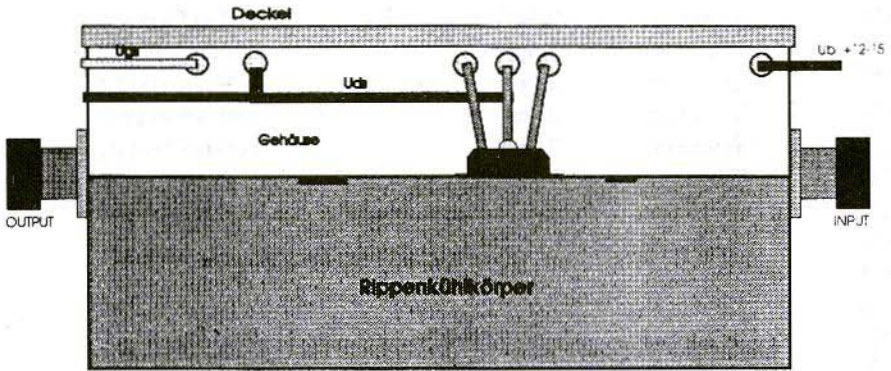


Fig.5a: Side View of a finished unit

Fig.5b: Component Layout

Deckel = Cover; **Gehäuse** = Cover; **Rippenkühlkörper** = Finned Cooling Body;
Mit der Platine & Folie verlötet = Soldered to Board and Foil;
Weißblechgehäuse = Tinplate Housing; **Kupferfolie** = Copper Foil;
Nut = groove; **Masseniete** = Solid Rivets; **Kühlkörper** = Cooling Body;
Hohlmete, durchkontaktiert = Hollow rivet, through-hole plated;
Netzteilplatine, senkrecht eingebaut = PSU board, vertically inserted



3. AMPLIFIER ASSEMBLY

The amplifier circuit is assembled on a Teflon board ($\epsilon_r = 2.33$) with the dimensions 146 mm. x 72 mm. x 0.79 mm.. For its part, it is screwed to an aluminium finned cooling body with dimensions of 147 mm. x 100 mm. x 40 mm., which acts as a fastening and a heat sink for the power transistors and voltage regulator (Fig.5a).

The DC voltage supply is mounted on a double-coated epoxy board, measuring 105 mm. x 20 mm. x 1.6 mm., internally soldered vertically to the longitudinal side of the housing (Fig.5b). Its circuit and structure correspond to the publications as per [6] or [1].

Fig.6 shows the wiring diagram, Fig.7 the components diagram, and Fig.8 the parts list for this power supply. The components are all mounted on the foil side, so that the earth surfaces have to be through-hole plated.

Grooves are milled in the cooling body, so that the drain and gate connections of the transistors can be soldered as flat as possible to the board. The grooves are laid out a little wide, to give a greater tolerance in the mounting of the transistors.

The Teflon board has a recess of 4.5 mm. x 17 mm. and two recesses of 6.5 mm. x 22 mm., into which the transistors are inserted and then screwed to the cooling body (see Fig.5). Between the board and the cooling body, there is also some copper foil (dimensions

148 mm. x 73 mm. x 0.08 mm.), which is later soldered to the tinplate housing. It improves the earth connection between the transistors, the board, the housing and the cooling body.

Before the board is installed, the earth surfaces must be through-hole plated using 2-mm. diameter hollow copper rivets. Here there should be 3 or 4 rivets per longitudinal side and 1 or 2 rivets per earth link (see Fig.5). The board is fastened to the cooling body by means of 8 M2 screws. The transistors need 2 threaded holes each in the baseplate for the source connection.

The tinplate housing (147 mm. x 72 mm. x 28 mm.) is provided with the appropriate holes and recesses before assembly. The housing is soldered together and soldered to the screwed-on board on the longitudinal sides. The soldered-on sockets are also screwed into the front faces of the cooling body.

The best approach is to assemble the components and bring them into operation in the following sequence:

- Assemble and incorporate the power supply board. The gate resistances (R4, R5) should already be soldered to the power supply for a better assembly!

Tip: To avoid regenerative feedback, the gate power supply connection for the transistor, T3, through the resistance, R6, may not go straight across the board, but must be taken round outside, like the drain power supply (see Fig.5).

- Install and wire up the 8 feedthrough capacitors (1 nF) and the blocking capacitors, C9 - C15, C17, C19.



- Insulated fastening and connecting of voltage regulator using feedthrough capacitors.
- Install and connect resistances (R7, R8, R9, R11, R12) on and to high-frequency board.
- Install trimmers (C1 - C6)

Tip: Ceramic trimmers of the Johanson 0.5 - 2.5 pF type are more suitable than Teflon trimmers, as they still give stable capacity values, even after repeated calibrations!

- Install chip capacitors (C7 - C10)

Tip: You should definitely use the very low loss ATC 100 porcelain type from Johanson.

- De-bugging the power supply (UG and UD)

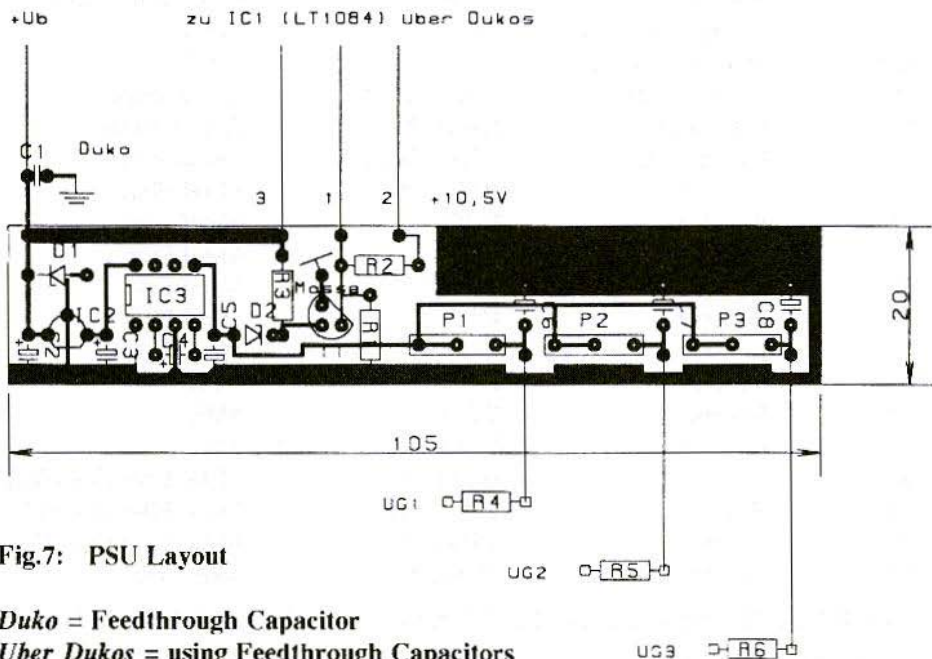
- Install GaAsFETs

- Set zero signal currents:
0905 - ID = 0.8A; 0906 - ID = 1.1A

4. READINGS

After calibration at 2,320 MHz, the prototype attained an output power of 11 Watts with a driving power of 120 mW. The measurement was carried out using an HP 432B Wattmeter and a 30 dB + 10 dB attenuator from Narda.

Fig.9 shows the amplifier's transfer characteristic. The compression area begins at an output power level of approximately 10.5 Watts - i.e. any



C1	Capacitor	1nF	Feed-Through
C2	Capacitor	10 μ F	Tantalum 16V
C3	Capacitor	10 μ F	Tantalum 16V
C4	Capacitor	22 μ F	Tantalum 10V
C5	Capacitor	22 μ F	Tantalum 10V
C6	Capacitor	10 μ F	Tantalum 10V
C7	Capacitor	10 μ F	Tantalum 10V
C8	Capacitor	10 μ F	Tantalum 10V
C9	Capacitor	0.1 μ F	Tantalum 10V
C10	Capacitor	0.1 μ F	Tantalum 10V
C11	Capacitor	0.1 μ F	Tantalum 10V
C12	Capacitor	10 μ F	Tantalum 16V
C13	Capacitor	10 μ F	Tantalum 16V
C14	Capacitor	10 μ F	Tantalum 16V
C15	Capacitor	100nF	
C16	Capacitor	1nF	Feed-Through
C17	Capacitor	100nF	
C18	Capacitor	1nF	Feed-Through
C19	Capacitor	100nF	
C20	Capacitor	1nF	Feed-Through
D1	Diode	ZD16	Zener
D2	Diode	ZD4.7	Zener
IC1	Voltage Regulator	LT1084	Low Drop TO247
IC2	Voltage Regulator	78L06	TO92
IC3	DC-DC Converter	ICL7660	DIL8
P1	Potentiometer	2.5k Ω (2k Ω)	Piher/Cermet
P2	Potentiometer	2.5k Ω (2k Ω)	Piher/Cermet
P3	Potentiometer	2.5k Ω (2k Ω)	Piher/Cermet
R1	Resistor	2k Ω (22K 2.2K)	Metal Film
R2	Resistor	270 Ω	Metal Film
R3	Resistor	10k Ω	Metal Film
R4	Resistor	470 Ω	Metal Film
R5	Resistor	470 Ω	Metal Film
R6	Resistor	470	Metal Film
R7	Resistor	470 Ω	SMD
R8	Resistor	470 Ω	SMD
R9	Resistor	470 Ω	SMD
R10	Resistor	3 Ω / 1.5W	Metal Film (3 x 10 Ω)
R11	Resistor	0.5 Ω / 1W	Metal Film (2 x 1 Ω)
R12	Resistor	0.5 Ω / 1W	Metal Film (2 x 1 Ω)
T1	Transistor	BC546B	NPN TO92

+5 1nF Feed-Through Capacitors for PSU from UG3 and LT1084, (see Fig.5)

Fig.8: PSU Parts List

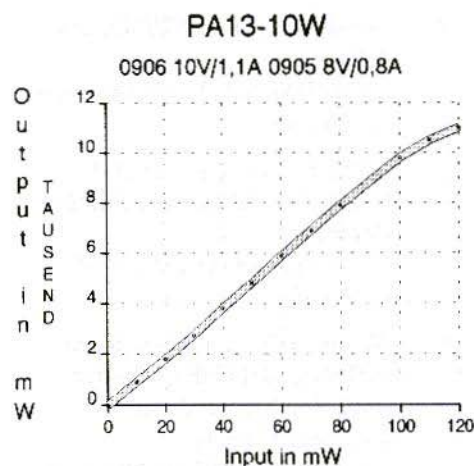


Fig.9:
Transfer Characteristic
for 10W PA



further increase in power leads to a considerable reduction in the inter-modulation interval and thus to signal distortion in linear mode.

Fig.10 shows the gain slope measured by means of an HP 8690B sweeper with 8699B at an input power of 50 mW and plotted against the frequency.

Here curve A shows the slope measured for an amplifier tuned to 2,320 MHz. Curve B shows the slope in a simulation of S21, as per Fig.1. The amplifier

consequently has a power band width of over 100 MHz. Its amplification drop to the limit frequencies is, of course, somewhat greater than in Curve B. The linear amplification of 20 dB attained deviates only slightly from the calculated values.

This amplifier can be used in the ATV range at 2,380 MHz - with rather less amplification for the same output power, of course. The author therefore developed an amplifier specially de-

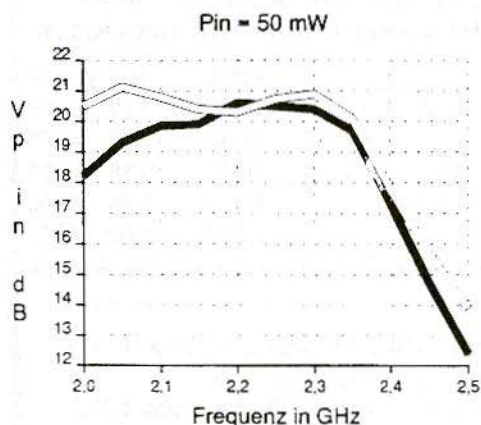
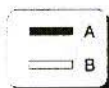


Fig.10:
Gain Slope plotted
against Frequency



signed for the ATV range, with a maximum amplification level app. 80 MHz higher. Another article in the near future will give details of the layout and the readings obtained.

Note: The PUFF CAD software package used in this project is available from KM Publications at the usual address. The price of the software at the time of publication of this article is £20.00 plus shipping at cost.

5. LITERATURE

- [1] Fleckner, H.: A Power Amplifier for the 13cm Band using GaAs Technology
VHF Communications 3/1994, pp. 130-141
- [2] Bertelsmeier, R.: PUFF-Design Software
Dubus-Info, vol. 18 (1989), no. 4, pp. 30 - 33
- [3] Lentz, R.E.: PUFF - a CAD Program for Microwave Stripline Circuits
VHF Communications 2/1991, pp. 66-68
- [4] Wedge, S.W., Compton, R. and Rutledge, D.: PUFF Computer Aided Design for Microwave Integrated Circuits
Available from KM Publications
- [5] Unger / Harth: High-Frequency Semi-Conductor Electronics
Hirzel-Verlag Stuttgart
ISBN 37776 0235 3
- [6] Kuhne, M.: High-Power GaAs-FET Amplifier for 9 cm.
Dubus-Info, vol. 20 (1991), no. 2, pp. 7 - 16

ADDITIONS TO OUR BOOK LIST

KM Publications now stocks a selection of ARRL books especially dealing with VHF and upwards and Antenna Design

	Price	UK	World
ANTENNA BOOK 17th Edition (c/w Software)	22.50	+3.30	+6.00
YAGI ANTENNA DESIGN	12.50	+1.50	+2.00
UHF/MICROWAVE EXPERIMENTERS MANUAL	16.00	+3.00	+3.75
UHF/MICROWAVE PROJECTS MANUAL	16.00	+2.50	+3.00
1995 ARRL HANDBOOK	22.50	+5.00	+7.25

Credit Card Orders +5% (for air mail delivery please enquire for cost)

KM Publications, 5 Ware Orchard, Barby, Nr.Rugby, CV23 8UF, UK

Tel: (0)1788 890365 Fax: (0)1788 891883

Email: vhf-comm@g6iqm.demon.co.uk or CompServe: 100441,377



Dr. Ing. Jochen Jirmann, DB1NV

New Software for the Digital Image Store for the DB1NV 010 Spectrum Analyser

Since the digital image store was first introduced at the beginning of 1991, the author has been informed of some suggestions for improvements, which have been reflected in the 2.04 software version now available.

The principle alteration is an HPGL plotter driver, so that there can be an output using pen plotters or LaserJet compatible printers. A few changes of detail were also undertaken and the program code was completely revised; e.g. the display mode with 2048 points of horizontal resolution has been deleted. The software is designed in such a way that the EPROM can be used in existing image storage equipment with minimal changes.

Here are some details of the functions provided for:

1. When switched on, the image storage equipment operates in graphic printer mode (EPSON compatible) and the screen generator is set to 8 x 10 boxes.
2. If another basic setting is desired, that can be obtained using diodes between the processor port P3.2 (pin-12) and ports P1.0 to P1.2 (pins-1 to 3). In this connection:

P1.0...|<...P3.2: The grid generator is wired up for 10 x 10 boxes.

P1.1...|<...P3.2:
When equipment is switched on or reset, output is set to HPGL.

P1.2...|<...P3.2:
Output on matrix printer in HP Thinkjet mode with 192 pixels/inch.

The diodes between P3.0, P3.1 and P3.2, used to preset the printer in earlier versions, had to be removed.
3. You can switch between the matrix plotter and the HPGL plotter at any time: hold the "Plot" key down and press "Reset" briefly: HPGL mode; hold down "Reference Memory" key and press "Reset": Epson mode; if

only "Reset" is pressed, then the diode at P1.1 determines the graphics mode.

4. The printer type is labelled through a "flashing code" output at P3.2. To this end, you can wire up an LED (don't forget the pre-resistance from 330 to 680 Ohms) from the "Plot" key as per +5 V. In the matrix printer mode, the LED comes on once for a long period after a reset or when plotting begins. In the HPGL mode, it gives three short flashes.
5. The digital mean value formation has been switched over. It is now carried out during the reverse saw-tooth phase. Since in any case the averaging is meaningful only at low scanning speeds, the time required for this carries no weight. The function is started by holding the "Normalise" key down and pressing

"Reset". During the averaging procedure, the measurement and the image output are stopped for a few milliseconds, which can be observed as a brief flickering in the image.

6. The reverse phase is now also blanked out using the X-A/D converter; to make this function more reliable, the converter input level should be set so high that the maximum control range is reliably scanned.

The new EPROM version can be obtained immediately from the publishers. In conclusion, the author would like to point out that exotic types of printer and plotter or looped-in add-on units such as intelligent printer multiplexers may malfunction. Neither the author nor the publishers can undertake to adapt individual printers, as this would need a lot of time and money!

SPECIAL OFFER

to VHF *Communications* readers only

23cm **M67715** Power Module 10mW in - 1.5W out

normal catalogue price £59.95 each

quote the following reference VHF COMM4/95 and get

them for **ONLY £30.00** plus VAT and p&p

Mainline Electronics, P.O. Box 235, Leicester, LE2 9SH.

Tel: 0116 278 0891 Fax: 0116 247 7551



Andreas Schaumburg, DF7ZW

A Simple DC-to-DC Down Converter for Amateur Radio Applications

This article is intended to make DC-to-DC converters a little more familiar and to stimulate others to follow the author's example. The converter can replace conventional linear adjustments in power packs and considerably improve their efficiency.

We are talking about a down converter with a converter integrated circuit at its core, which requires scarcely any external connections. A higher DC input voltage is converted into a stabilised lower DC output voltage without potential separation. Due to lower losses, the power pack can be made more compact, with smaller cooling bodies and a weaker 50 Hz transformer. The effi-

ciency goes up by app. 90% with max. output current 5A, which can not be exceeded because of internal current restriction. The converter integrated circuit can thus be considered as the successor to the widely-used linear regulator from the 78XX range.

1. THE BASIC CIRCUIT WITH INDUCTANCE CALCULATION

The principles and the basic circuits of switching power packs have already been dealt with by Jochen Jirmann,

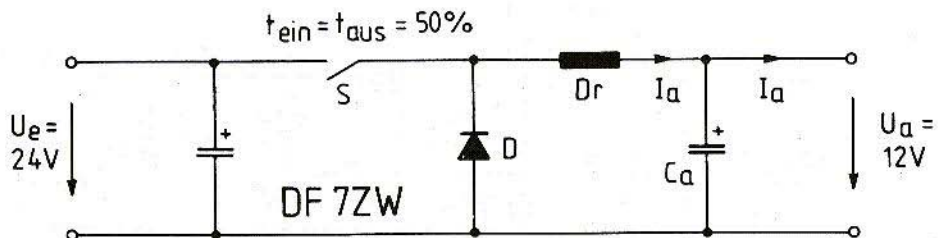


Fig.1: Basic Circuit $ein=in$; $aus = out$

DB1NV, in VHF Comm's 2/1985, pp. 79-93. The circuit described below represents a secondary converter without potential separation. The circuit's function is shown in the outline wiring diagram (Fig.1). The components have been assumed to be ideal. The input voltage, U_e , amounts, for example, to 24V, and the output voltage, U_a , to 12V, with an output current of 5A. The mark-space ratio of the switch is now exactly 50%. The output current (5A in our example) flows through the choke.

An ideal choke means an infinitely high inductance, and the DC current flowing through it is even. If the switch is closed, the diode, D, locks, and there is a drop of 12V at the choke, D_r . The inductance is now magnetised. If the switch is opened, the recovery diode, D, is now conducting, so that again there is a drop of 12V at the choke, D, but preceded by a negative sign. The inductance is now demagnetised. With a real choke, which has a finite inductance, this leads to current ripple. The inductance level is calculated using the following differential equation:

$$UI = L \cdot (di / dt)$$

When the equation has been transposed and linearised, we obtain:

$$L = UI \cdot (\Delta t / \Delta i) = 12V \cdot (7\mu S / 1A) = 84\mu H$$

The switching frequency of the IC is 72 kHz, so that, with a mark-space ratio of 50%, the on-transition time (Δt) is $7\mu S$. The current ripple (Δi) amounts to 20% of the DC current which is flowing in the choke - i.e. 1 Ass. A choke is required with an inductance of app. $0.1\mu H$, with a DC current pre-magnetisation of 5A. Only cores with a greatly reduced permeability can be considered for this application. Toroidal cores are used with a permeability, μ_r , of app. 100, or ferrite cores with an air gap. In the prototype, a KOOL Mu Powder Core, type 77206, from Magnetics (obtained from BFI-IBEXSA, Eching) was used, with $\mu_r = 125$ and external d., $D = 21.1$ mm. Material 26, from Amidon, with $\mu_r = 75$, should be suitable. The selection criterion is the maximum energy storage of the core, given as $L \cdot i^2$ in the manufacturer's data sheet (to be physically correct, it should have been: $EI = 0.5 \cdot L \cdot i^2$). The type 77206 core has an $L \cdot i^2$ of $1.3mHA^2$, according to the data sheet. In practise,

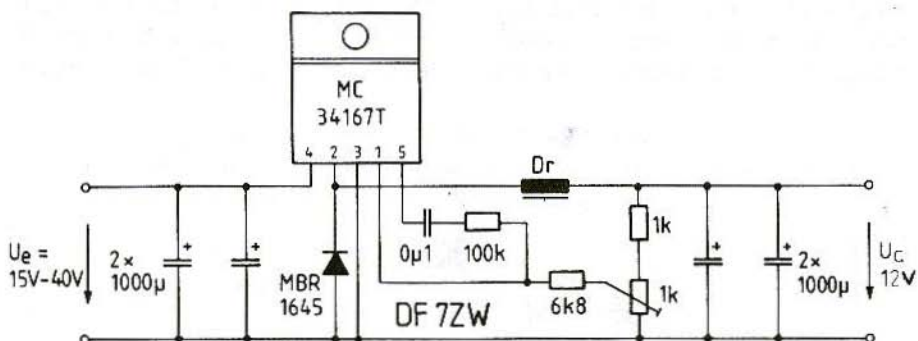


Fig.2: Circuit Diagram of the Switching Power Pack

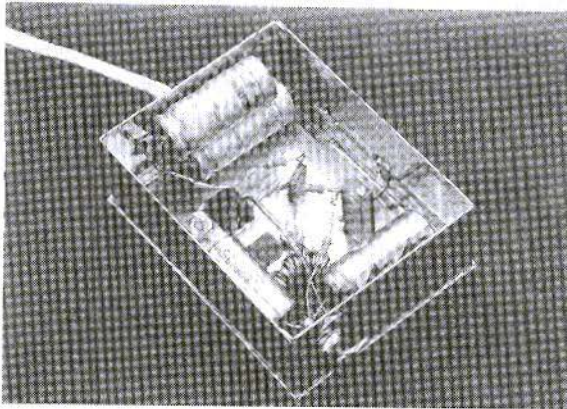


$L \cdot i^2 = 5A^2 \cdot 0.1 \text{ mH} = 2.5\text{mHA}^2$. Saturation arises easily with these dimensions, but it is not critical. The core was coiled in 41 windings of 1.18 mm. copper lacquer wire, which gives an inductance of $0.115\mu\text{H}$ for a 4.6Amm^2 current density. Up to 90% DC current is flowing in the choke, so that the skin effect plays scarcely any part, and no high-frequency wire is required for the winding.

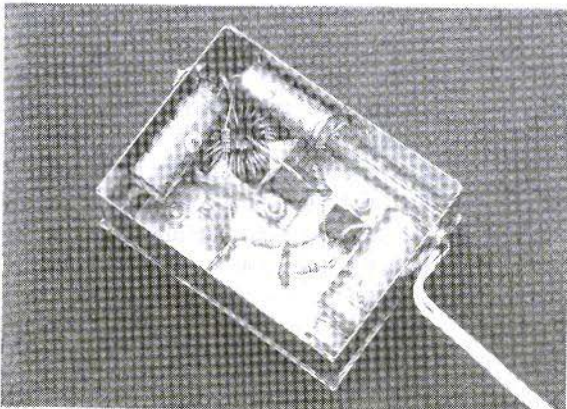
2.

CIRCUIT ASSEMBLY

Fig.2 shows the wiring diagram for the switching power pack. The circuit is wired up as an "open-air assembly" in a tinplate housing. Inputs and outputs are created by means of feedthrough capacitors. The converter IC used is type MC34167T from Motorola. The difference between the input and output



Fig's.3a & b:
Two views of a Prototype Converter



voltages should be not less than min. 2.5V. The max. converter input voltage, according to the data sheet, is 40 Volts.

For an output current of only 3A, Motorola has the "little brother", MC34166T, in its range, which is pin-compatible. Similar types of converters for max. 3A can be obtained from National-Semiconductors.

An MBR1645 Schottky diode is used as the recovery diode, D, in the TO220 housing. Electrolytic capacitors with a low internal resistance should be used as input and output capacitors, and several of them should be wired up in parallel, depending on the electromagnetic compatibility requirements.

Fig.3 shows the author's prototype. With app. 90% efficiency and full output current, you can expect a power loss of app. 8 Watts. So only a relatively small cooling body is needed.

3.

PUTTING CIRCUIT INTO ACTION AND ELECTROMAGNETIC COMPATIBILITY

To put the circuit into action, it should be powered from a laboratory power system with current restriction. The current restriction prevents the converter from being destroyed in case of wiring errors. The output voltage, U_a , is set using the $1k\Omega$ potentiometer. A current ripple value of $1.8 A_{SS}$ was measured by means of a current clamp.

This value is somewhat larger than the calculated value, because the choke is easily driven in saturation. With a larger core, e.g. type 77310, with $D = 23.6$ mm. and $Li^2 = 2mHA^2$, the current ripple falls still further. The current blocks which are normal for the filter capacitors are removed - there are thus no longer any electromagnetic compatibility problems in the input circuit.

Various pieces of radio equipment were connected up for the converter's test run, and the transmission signal was monitored by a spectrum analyser. In no case was the 72 kHz switching frequency recognisable in the output spectrum of the transmitter. Moreover, the converter is in the position of being able to adjust out a 100 Hz hum from the screen electrolytic capacitor of the rectifier.

4.

CONCLUSION

The author subsequently fitted various linear-regulated power packs with the above circuit for converter operation. The cooling bodies for the previous series pass transistors could be dispensed with, since with the converter's low power loss the power pack housing is usually sufficient for the cooling. The circuit is also outstandingly suitable for portable use, e.g. to supply power to GaAsFETs for the microwave range which operate at 5 to 7 Volts, from a supply voltage of 12V.



François Cronauer, LX1DU

First Amateur Cloud Scatter Beacon in Europe

A series of experiments carried out by LX1DU over a long period of time yielded interesting results in relation to the propagation of signals at 10 GHz.

I. INTRODUCTION

Approximately 400 link-ups were carried out as part of a series of experiments by LX1DU in relation to the propagation of microwaves in the 10 GHz range. After every link-up, notes were made regarding the time, temperature, atmospheric humidity, air pressure, cloud cover, and, if applicable, mist, rain, and the field strengths of the responding station and of various beacons at 23 and 13 cm.

Later the data was fed into a PC and used to create diagrams. Analysis revealed that outstanding field strengths could be obtained at 10 GHz in bad weather, whilst the 23cm or 13cm

beacons could be heard only very faintly, or not at all!

The results show that the 3cm band is clearly a "bad weather band". The

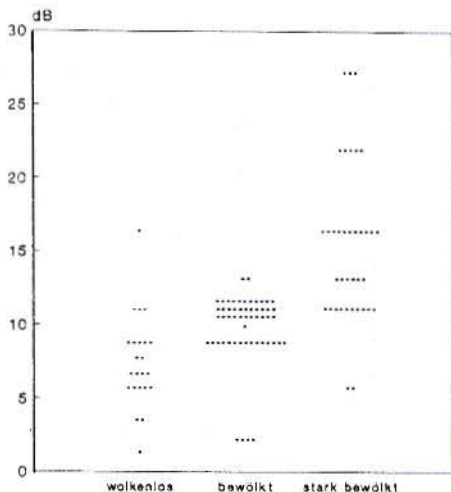


Fig. 1:
The Evaluation of the series of experiments shows a marked increase in the Field Strength with heavy cloud cover.

Wolkenlos = Cloudless;

Bewölkt = Cloud cover

Stark bewölkt = Heavy cloud cover

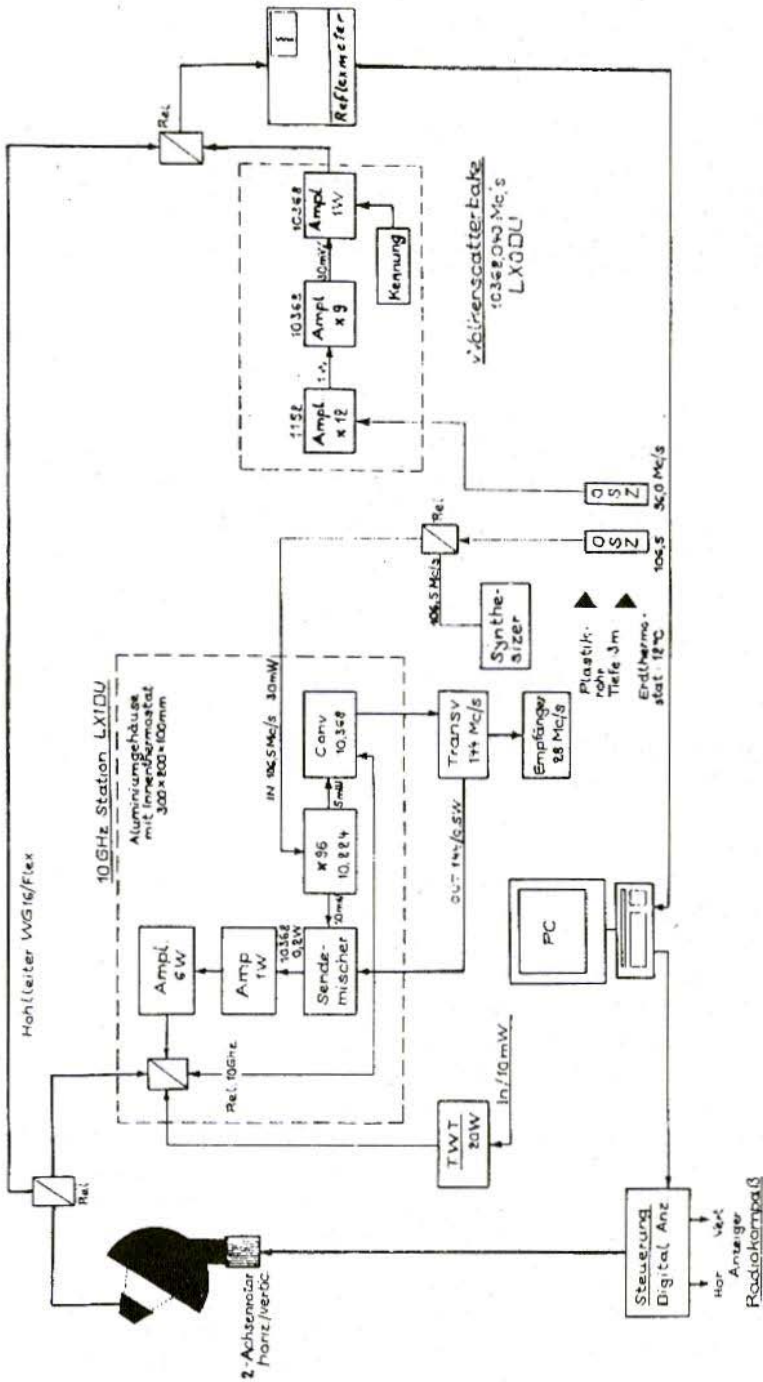


Fig.2: Block Diagram of the Station and Beacon's LX1DU and LX0DU



Series of tests on Propagation of Microwaves in the 10 GHz range.

Technical data for LX1DU

Dish: 1.25 m ϕ
 Power: 5 W
 Converter: 1 dB Noise Figure
 Locator: JN29XM
 Height ASL: 360 m

Technical data for DL9SH

Dish: 0.85 m ϕ
 Power: 1 W
 Converter: 2 dB Noise Figure
 Locator: JN49DN
 Height ASL: 124 m

1	2	3	4	5	6	7	8	9	10
Date 1991	Time	LX1DU dB	DL9SH dB	Press M'bar	Hum'y %	Temp °C	Cond's 23cm	Cloud	Rain
28.09	22.00	5.0	2.0	975	90	+12	1	0	0
29.09	16.00	6.0	2.0	978	90	+14	1	0	0
30.09	12.50	10.0	5.0	980	92	+19	1	2	0
30.09	22.00	5.0	2.0	985	91	+10	1	0	0
01.10	07.10	7.0	2.0	975	90	+10	1	0	0
01.10	22.00	7.0	2.0	990	94	+ 9	1	0	0
03.10	07.00	8.0	2.0	1004	92	+ 8	1	0	0
04.10	22.00	20.0	12.0	995	85	+10	1	2	1
06.10	22.00	10.0	2.0	990	85	+14	1	0	0
07.10	07.00	10.0	1.0	992	85	+12	1	0	0
07.10	22.00	10.0	1.0	993	85	+12	1	0	0
08.10	22.00	8.0	1.0	992	85	+13	1	0	0
09.10	07.00	8.0	1.0	990	80	+13	1	0	0
09.10	22.00	8.0	1.0	992	82	+12	1	0	0
10.10	07.00	12.0	6.0	991	80	+12	1	1	1
10.10	22.00	12.0	7.0	991	80	+11	1	1	1
11.10	07.00	10.0	4.0	990	80	+13	1	1	0
11.10	22.00	8.0	3.0	985	85	+13	1	1	0
14.10	07.00	10.0	2.0	984	85	+12	1	1	0
14.10	22.00	10.0	2.0	985	83	+13	1	1	0
15.10	07.00	10.0	4.0	987	80	+12	1	1	0
15.10	22.00	8.0	1.0	989	80	+13	1	0	0
16.10	22.00	10.0	3.0	986	82	+13	1	2	0

Notes: Column-8 23cm Conditions: 0 = nothing received; 1 = normal; 2 = good
 Column-9 Cloud Cover: 0 = cloudless; 1 = light cover; 2 = heavy cover
 Column-10 Rain: 0 = no rain; 1 = light rain, 2 = heavy rain

Fig.3: Extracts from the detailed Test Report

diagram in Fig.1 clearly shows that, even with light cloud cover, an increase in field strength of up to 10 dB can be obtained, and with heavy cloud cover there is very often an increase of up to 25 dB. We should not overlook here that the two stations were almost 200 km. apart.

As the results of this long-term study can be interpreted as showing a direct link between the increase in field strength and the cloud cover, it was an obvious idea to construct a beacon which could permanently beam a signal into the clouds.

The initial cloud scatter beacon experiments were unsuccessful. As later became clear, the power was too weak. It was not until a test rig was set up with a parabolic reflector with a diameter of 1.3 m., a gain of 40 dB, and a beacon output power of 500 mW that success was achieved. The beacon has been operating for months at 10.368040 GHz, under the call sign LX1DU. Its signals have already been heard, with good field strengths from various QRA locators.

2. SCATTER BEACON ASSEMBLY

Fig.2 makes it clear how the beacon was assembled. A remote 96 MHz crystal oscillator, with a power of app. 10 mW, powers a twelve-fold multiplier (through a thin coaxial cable) with a subsequent amplifier, which thus

yields app. 1 Watt at 1,152 MHz. The subsequent nine-fold multiplier brings the signal up to 10.368 MHz. It is now amplified again, through a power amplifier, to 0.6 Watts. The signal is fed to the parabolic reflector, by means of wave guides, type WG/16, with an overall length of 12 m., and of a series of special microwave relays. In order to obtain very good long-term stability, the crystal oscillator was sunk app. 3m deep into the ground in a closed plastic tube with a diameter of 50 mm.. At this depth, the temperature is already relatively constant at 12.5 degrees. In order to make this beacon complete, it also has a call sign transmitter for the location and transmits call signs in Morse code.

3. SCATTER BEACON'S FUNCTION

In conjunction with a computer and a two-axis rotor (resolution 0.2 degrees), a reflection measurement unit searches for a strongly reflecting cloud formation. The information on the degree of reflection is fed to the computer, which now makes a fine correction. After precise setting, the rotor is automatically stopped, and the reflection measurement unit is separated from the antenna. The beacon signal is now fed to the parabolic antenna through a wave guide switch and beamed into the clouds. If the signal is heard on the 10368.040 MHz frequency, we know that cloud scatter is present. The an-



tenna is aligned for maximum field strength. Now we can pick up scatter links through this cloud formation. If there are no clouds in the sky, the beacon can scarcely be heard. Very strong reflections have been measured in the direction of the Moselle valley (Az 63°, El 3°). It seems that the cloud pattern along the Moselle valley plays a decisive role. Not all clouds have such good reflection characteristics. Thick black storm clouds are the most suitable. The range within which link-ups can be carried out depends on the height of the cloud formation.

4. SUPPLEMENT

If you have weather images from Meteosat available, ideally in time-lapse form, the cloud patterns, wind direction, speed and approximate arrival time of cloud formations can be estimated.

MITSUBISHI POWER FET'S

The 090 series of these devices is now available from
Mainline Electronics

These devices are now being used in many VHF
Communications projects and designs from elsewhere
Contact Mainline for full details of stock and the latest
competitive prices

Mainline Electronics, P.O. Box 235, Leicester, LE2 9SH
Tel: (0)116 278 0891 Fax: (0)116 247 7551

ARRL QST Magazine

Now Available from KM Publications
£3.50 per issue p&p UK £1.00; Overseas £1.80

KM Publications, 5 Ware Orchard, Barby, Rugby, UK
Tel: (0)1788 890365 Fax: (0)1788 891883



Norbert Kohns, DG1KPN

Digital Display for the Logarithmic Detector Amplifier from DJ4GC

While building the logarithmic display amplifier from DJ4GC [1], I got the idea of replacing the analogue display instrument by a digital display using a data processing module.

1. GENERAL REMARKS

There are many arguments in favour of a digital display for this application. Here are some of the advantages:

- It is no longer necessary to draw a scale for the indicating instrument
- The resolution is increased to 0.1 dB
- Values can be read off more easily
- Automatic preceding sign display
- In cases of diode replacement or faults, only the replacement equipment needs to be calibrated

Experiments with the tried and tested ICL7106 gave excellent results, which seemed to show that it made sense to use this integrated circuit.

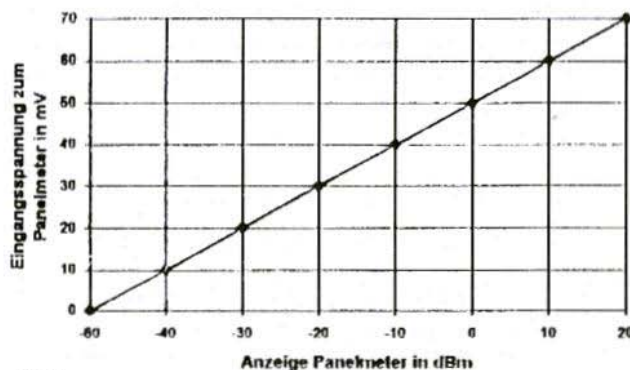


Fig.1:
Linear Relationship
between Input Voltage
and DVM Display Value
*Eingangsspannung zum
Panelmeter = Input
Voltage to Panel meter
Anzeige Panelmeter =
Panel meter Display*

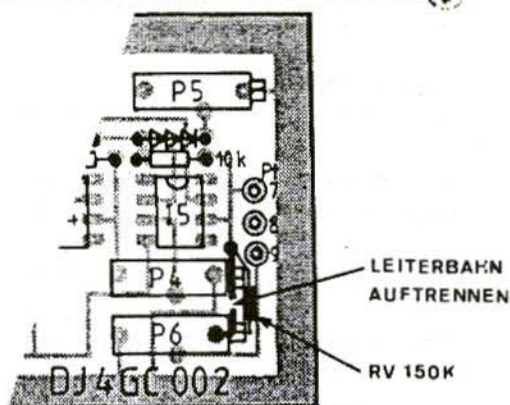
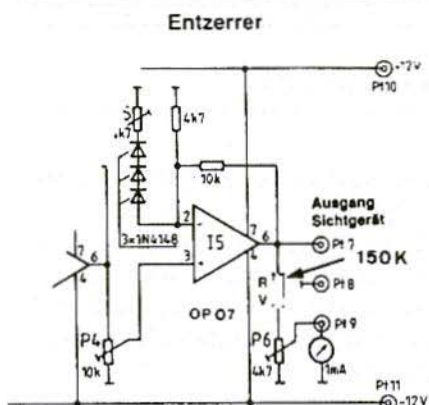


Fig.2a: Expansion of DJ4GC Circuit Fig.2b: Modifications to PCB
Entzerrer = Tone Control; *Ausgang Sichtgerät* = VDU Output
Leiterbahn aufrennen = Cut Track

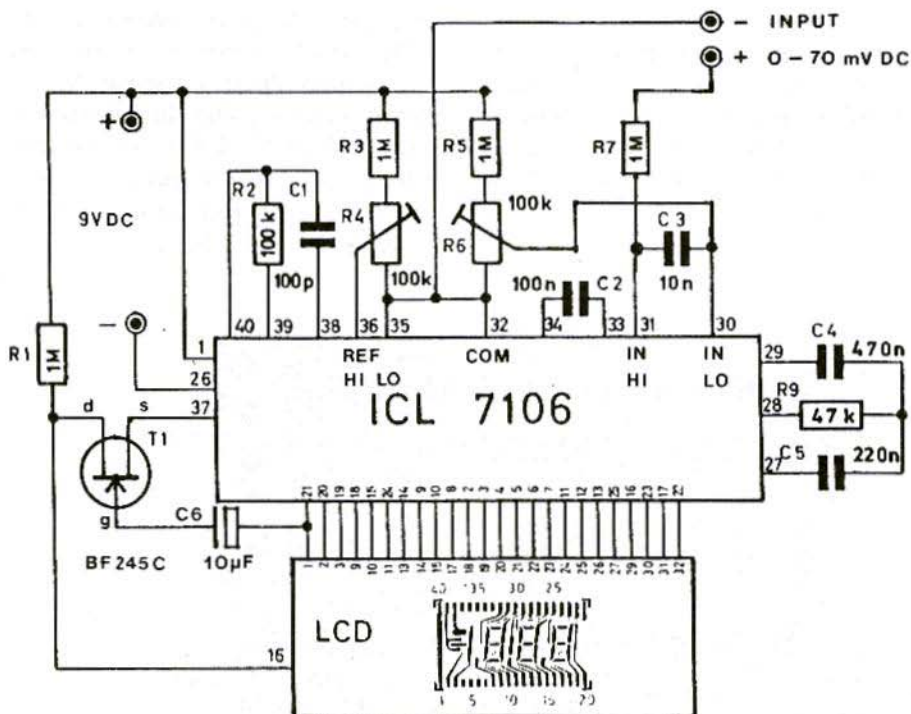


Fig.3: Circuit Diagram of the Digital Display

2. THE CONCEPT

Fig.1 shows the inter-connections between the input voltage of the DVM module and the display needed on the display unit. The input voltage (0 to 70mV) is obtained by inserting a 150k Ω resistance between output 15, pin-6 and the trimmer, P6 (Fig.2). As the diagram in Fig.1 shows, the DVM has to display -50.0 dBm at an input voltage of 0 Volts. Likewise, the display must read 00.0 if the input voltage is 50 mV.

The ICL 7106 offers the advantage that you can also obtain a zero reading for any input voltage value you like. This offset in the display is obtained by feeding in the variable input voltage - i.e. the measurement value - between "Input High" and "Common", and the offset voltage between "Common" and "Input Low".

3. THE CIRCUIT

The external wiring of the ICL 7106 for our application is shown in Fig.3. You need only a pair of external resistances, some capacitors and a transistor. A current model of a 3½ character LC display with 40 connections is used as a display unit.

4. THE ASSEMBLY

As regards the power supply for the DVM module, remember it must be isolated from the power supply for the display amplifier, since the "Common" input of the ICL 7106 is not identical with the earth, and is thus not at earth potential. The current consumption for 9 Volts DC is about 2mA.

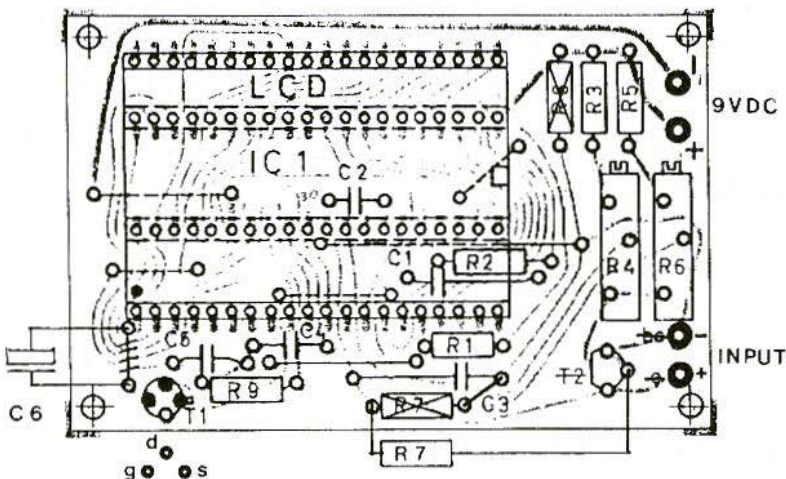


Fig.4:
Component
Overlay

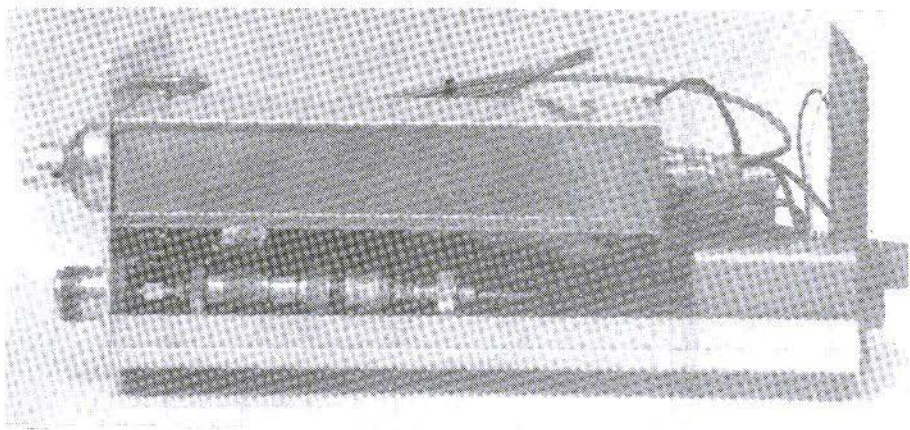


Fig.5: Side View: The built-in Diode Detector can easily be seen underneath.

To increase the stability of the circuit, only metal film resistances are used. This is why the OP07 is used in the offset and tone control stage.

If the logarithmic detector amplifier is assembled new, it is initially calibrated as described in the instructions from DJ4GC. Only after successful calibration should you connect the 150k Ω voltage multiplier in series with P6. For this purpose, the track from pin-6 to pin-15 is carefully cut through and the voltage multiplier is soldered to the underside of the board by means of the cut track (Fig.2a). With the input to the DVM module short circuited, set R6 in such a way that the display reads exactly -50.0. If we feed in +50 mV with the correct polarity at the input of the DVM module, we can use R4 to set the display to 00.0.

The entire calibration procedure should be repeated until no further improvement can be obtained. To obtain better long-term stability, is it advisable to subject the equipment to an endurance

run for app. 4 weeks, and then optimise the calibration again. Naturally, the accuracy depends on the diode detector used and the measuring equipment available. I myself have built two of these assemblies and obtained the following accuracy levels:

Range -10 to +10 dBm, app. 0.2 dB,
and app. 0.5 dB for the entire range.

I have been able to obtain these values for two years, following a fifteen minute warm-up period, without needing to re-calibrate the equipment. Later versions have given comparable results.

For the DVM module (Fig.3), the circuit of a digital thermometer [2], the components drawing of which is shown in Fig.4, was modified.

It has proved useful to incorporate the diode detector into the housing, to avoid noise interference through the feed cable (see Fig.5). This measure markedly increases the stability of the circuit without an input signal (display at app. -53 dBm).

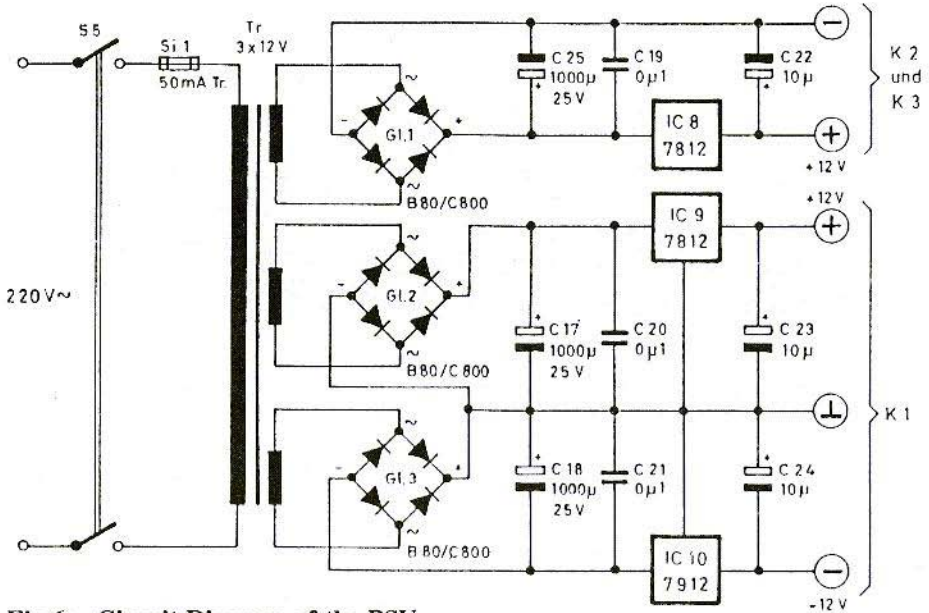


Fig.6: Circuit Diagram of the PSU

5. POWER SUPPLY

Fig.6 shows an example of a suitable power pack. Here the well-known regulators from the 78xx and 79xx ranges

are used to stabilise the voltages. Board layouts and components drawings can be used, with slight changes (IS8 is replaced by a 7809). The finished board is incorporated into a tinfoil housing for screening purposes.

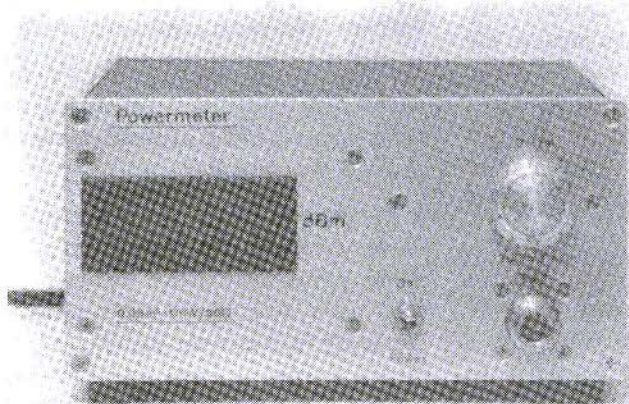


Fig.7:
Front View of the
Prototype

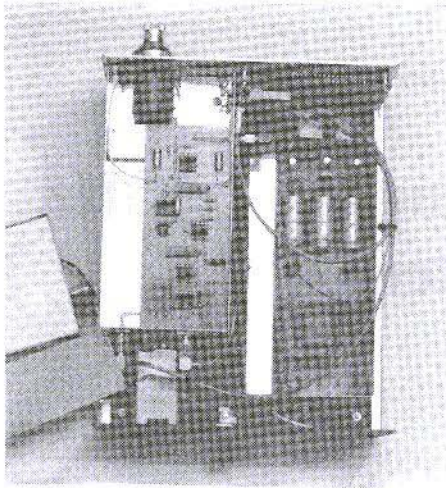


Fig.8:
Interior view of the
Prototype

6. PARTS LIST

Digital Voltmeter:

R1, R3, R5, R7	1 M Ω 1%
P9	47 k Ω 1%
P2	100 k Ω 1%
P4, P6	100 k Ω , helipot
C1	100pF
C2	100nF
C3	10nF
C4	470nF
C5	220nF
C6	10 μ F
T1	BF245C
IC 1	ICL7106
IC 2	LC display

Power pack:

C17, C18, C25	1000 μ F / 35V
C19, C20, C21	100nF / 100V
C22, C23, C24	10 μ F / 35V
IC8	7809
IC9	7812

IC10	7912
G1-G3	B80 C800 poly-directional
Transformer	220V, 3 x 12V / 3.5VA
1	fuse carrier

7. LITERATURE

- [1] Carsten Vieland DJ4GC
50 Ω Wideband Detectors
VHF Communications 2/1988,
pp. 111-125
- [2] Digital Thermometer
ELV-Journal, no. 2 / 1980
- [3] Power Supply
Elrad 1985, nos. 7/8
- [4] Maxim Data Book, no. 1/1986
ICL7106



Angel Vilaseca, HB9SLV and Jean-Pierre Morel, HB9RKR

The World's Smallest 10 GHz ATV Transmitter

The availability of cheap surplus GaAsFETs in latter years has made a lot of microwave experimenting possible for amateurs. This article describes a new kind of amateur 10 GHz low-power transmitter, using a surplus GaAsFET, mounted on a tiny piece of Teflon/Glass PCB, giving a wideband FM TV signal.

As many microwave oriented amateurs, we began back in the 80s using Gunn diodes in waveguide assemblies. These, providing they were home-built using cheap surplus diodes, were very cost-effective when compared to commercial transceivers (e.g. the Gunnplexer). The main disadvantage was the plumbing. It took a lot of time and a fairly well tooled workbench to build waveguide-based designs. For instance, some parts, like the screws used to hold the diodes, could only be made using a lathe.

However, if you were ever drawn away from the old 10 GHz band by the mechanical difficulties this article is for you. The 10 GHz transmitter described here could hardly be simpler.

1. THE GaAsFET OSCILLATOR

Trying to design a GaAsFET oscillator with the software CAD package PUFF, the computer program previously described in VHF Communications (issue 3/1991 pp. 66-68), we first considered a design similar to the one in Fig.1.

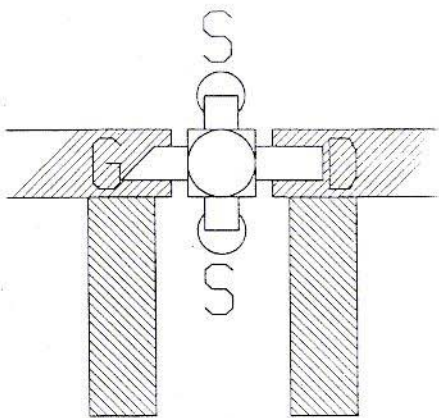


Fig.1: A GaAsFET Oscillator



As in many oscillators the oscillation takes place if there is an adequate feedback from an amplifier's output to its input. In the oscillator in Fig.1 the feedback is provided by the two close-coupled stubs connected to the gate and drain microstriplines. The source terminals of the GaAsFET are connected to the groundplane.

1.1 Making the Oscillator Radiate

Any conducting patch etched on a PCB radiates a part of the energy it is fed with. If the dimensions of the patch are small in terms of the wavelength of the signal then little energy is radiated. As the patch dimensions increase, radiation increases too, until a $\lambda/2$ patch dimension is reached. This is when radiation efficiency is at its peak.

This principle is not unknown to us, Yagi antenna elements are also of-the-order-of $\lambda/2$ long (Fig.2) and they are particularly efficient when it comes to radiating energy from transmitters! Radiation from microstrip elements is used in so-called Microstrip Antennas.

What we tried to achieve here was to combine the design of the previously mentioned oscillator with a microstrip antenna. Two microstrip antenna

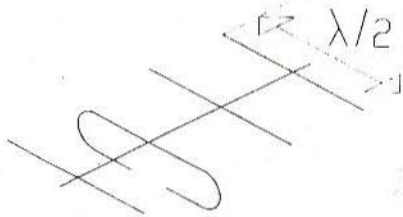


Fig.2: $\lambda/2$ Yagi Antenna Elements

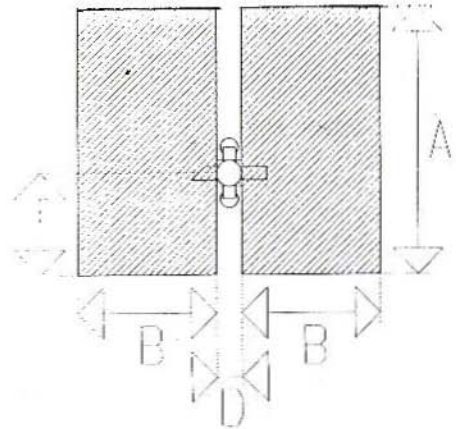


Fig.3: The Final Oscillator Design

patches were designed close-coupled to each other, the GaAsFET input (gate) was connected to one and the output (drain) to the other, thus obtaining the following design shown in Fig.3.

We decided to make both patches the same dimensions for our first attempt. In fact this is questionable, because if the two patches radiate with opposite phases then their respective radiations would cancel each other out. Perhaps a more in-depth theoretical (and mathematical) approach would be needed here.

However, experimentation showed that some radiation did take place. In fact, some mutual cancellation from the two patches can be desirable, if it is thought of as being equivalent to limiting the output coupling of a conventional oscillator.

If all possible energy is coupled out of an oscillator, its stability will be poor, because its characteristics will be affected by the circuit it is coupled to.

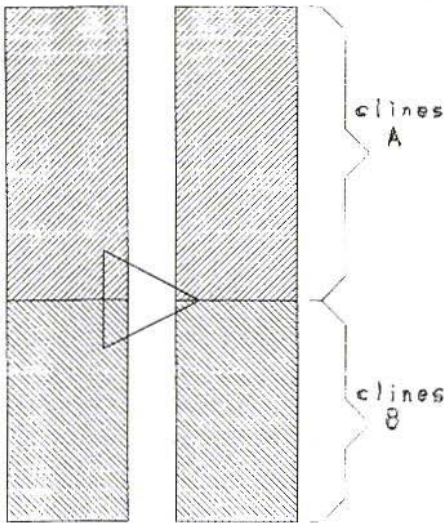


Fig.4:
For PUFF the oscillator is an amplifier with two pairs of coupled lines connected end-to-end. Various A and B lengths were tried, with the overall length $A+B$ remaining $\lambda/2$.

2. DESIGNING THE PCB

Fig.3 shows the four dimensions that must be decided upon. The circuitry was input to PUFF in the following manner.

1. The coupled lines A and B were chosen with the same low impedance, meaning that the lines were broad, as with a microstrip antenna patch. The dimension $B+D+B$ should be equivalent to about a half wavelength to maximise radiation.
2. To generate enough feedback for the oscillation to occur, the patches were chose with a tight coupling, which means close to each other. This determines dimension D.

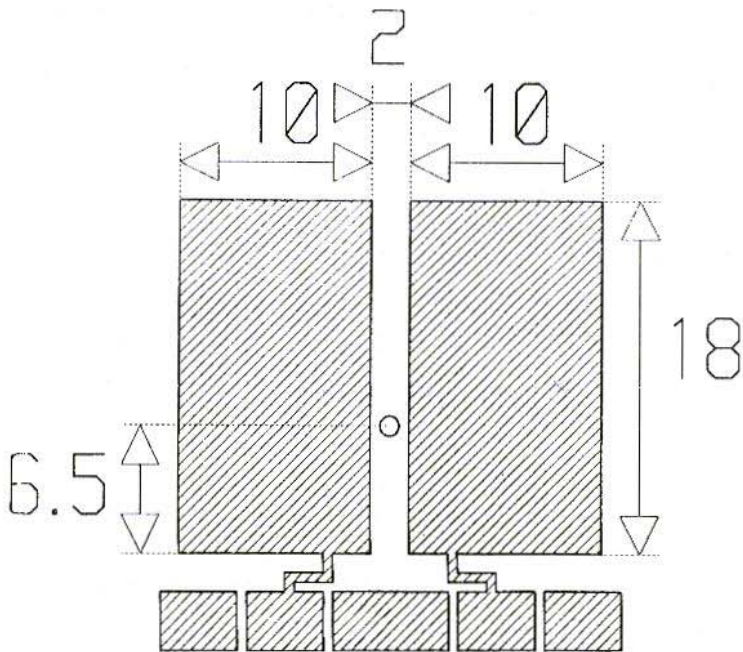


Fig.5a:
The PCB
Layout

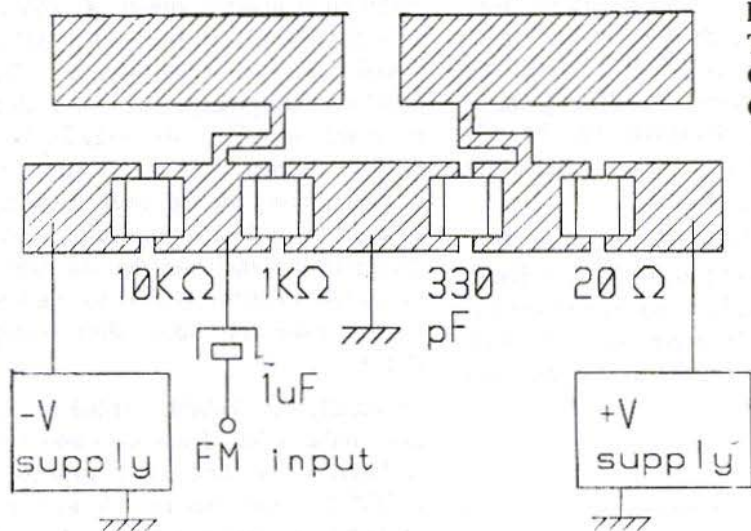


Fig.5b:
The
Component
Overlay

3. The overall electrical length of both lines placed end-to-end (A) was chosen at about $\lambda/2$ to maximise radiation. The point at which the GaAsFET was attached to the two patched (dimension C) was searched for using PUFF, by trial and error, so that feedback was as high as possible.

Finally, we decided to start experimenting with the PCB pattern shown in Fig.5a. The component overlay is shown in Fig.5b.

The test setup is shown in Fig.6. For an antenna we used a parabolic reflector, an IKEA dish, sold as a lamp, available cheaply in furniture shops. The diam-

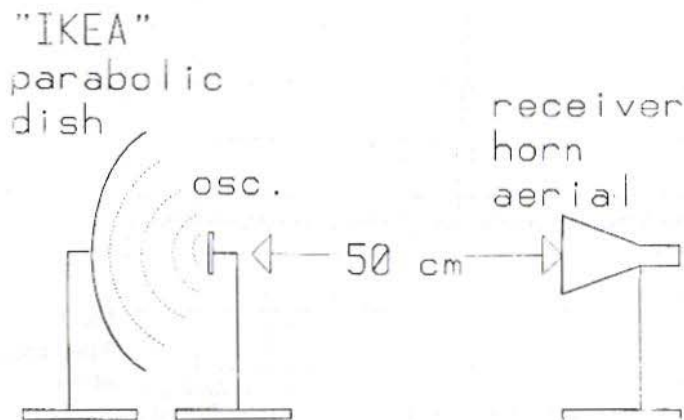


Fig.6:
The Test Setup

eter of the dish is 40cm and its focal length is rather short, at about 11cm., so F/D is low at 0.27. The oscillator was simply placed at the focal point so that it would illuminate the dish. No more *Penny Feed* - how is this for simplicity?

The GaAsFET we used was a Red Spot from Birkett's (J.Birkett, 25 The Strait, Lincoln, LN2 1JF, UK). Dimensions D and B (Fig.3) were held constant throughout the tests at B = 10mm and D = 2mm.

3. TESTING

For our first test we made A = 18mm and C = 6.5mm. With a positive supply

Active radiating element

of 4V and a negative supply of -3.5V Id was 23.4mA and we received a -3dBm signal with our horn antenna. The oscillation frequency was lower than predicted at 9.712 GHz (Fig.7). The received signal was best with the oscillator being shifted away from the focal point, at 16.2cm instead of 11cm. This probably indicates that the radiation angle from the PCB is too narrow to illuminate the whole dish evenly (Fig.8).

Eventually the GaAsFET failed (it did draw quite a lot of current!) and was replaced by a first class expensive CFY18-23 from Siemens. A was left unchanged at 18mm and D was tried at 7mm. The received signal was much lower at -17.3dBm. With D = 8.5mm the oscillation stopped. Most interesting was the fact that this small change in D brought the frequency almost 1 GHz higher at 10.653 GHz.

Redspot

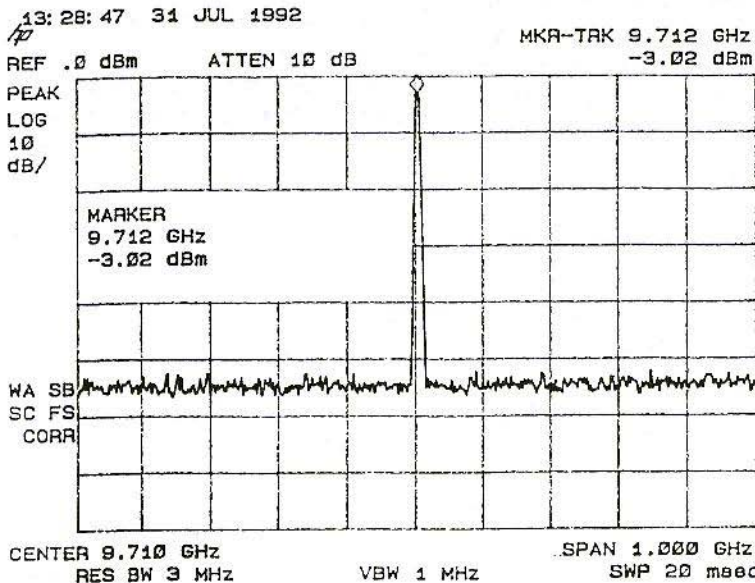


Fig.7:
The Signal
at the
Receiver

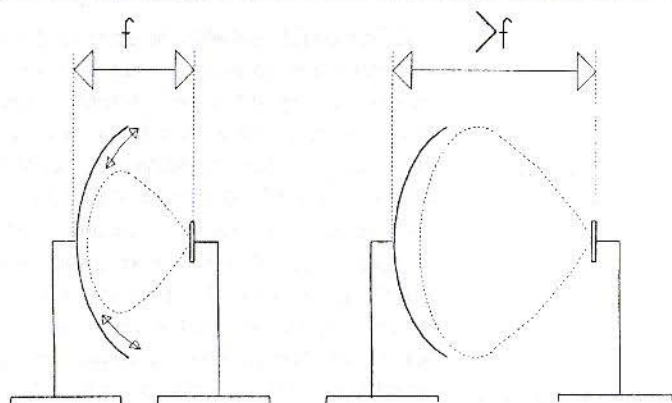


Fig.8:
If the Oscillator is placed further from the Parabola than the Focal Length it illuminates the Dish more evenly.

We replaced the CFY18-23 with a new red-spot GaAsFET with D left at 7mm and the frequency remained the same, so it really seems that the frequency shift comes from modifying D rather than changing the GaAsFET.

To lower the frequency down into the amateur band we fitted two small pieces of copper foil to the ends of both patches, increasing the A dimension to 19mm. This brought the frequency to 10.293 GHz with a positive supply of 3.5V and a negative supply of -4V, Id was 16.5mA.

Figure 9 shows the received signal when the oscillator is frequency modulated

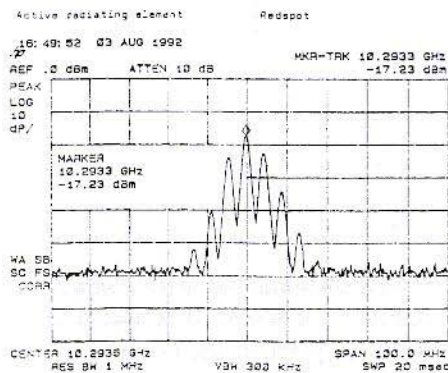


Fig.9: Output when Oscillator FM'd

lated by injecting a 4.5 MHz signal at the gate. Linearity is acceptable. Modifying the power supply voltage did not change the drain current much, but the frequency did change but non-linearly.

+ve	-ve	Id	Frequency
+3.0V	-4.0V	1.5mA	10.363 GHz
+3.5V	-4.0V	16.5mA	10.354 GHz
+4.0V	-4.0V	17.5mA	10.376GHz

The received signal was strongest at -17.23dBm when the PCB was set at 13.5cm from the dish. The cross-polarisation attenuation was rather high with a maximum of 30dB. The total radiated power was estimated at about 1mW. Replacing the circuit-under-test with a Gunn transmitter of 1mW known power output gave the same signal on our test bench.

We further tried to decrease D to 5mm. This sent the output power up to about 3dB and the drain current down to 11.4mA. The oscillation frequency also went down to 10.180 GHz, which allowed us to remove the two pieces of copper foil we had previously fitted to the patch ends. This brought the frequency back up to 10.430 GHz.

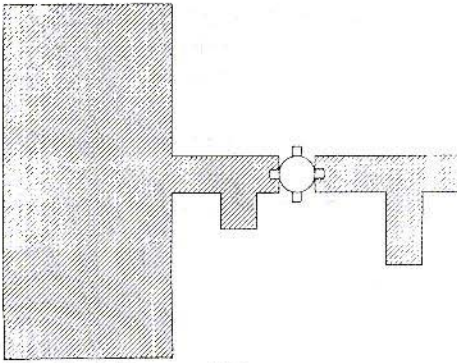


Fig.10: A Preamplifier connected to a Microstripline Antenna

4. CONCLUSIONS AND FURTHER DEVELOPMENTS

Well, this is it, we have made a 10 GHz ATV transmitter using only six components - possibly a Guinness Book record? Stability was good with only small frequency shifts caused by moving objects near to the transmitter. Although we did not try it, temperature

stability could probably be enhanced by enclosing the transmitter between two sheets of expanded polystyrene. This material has very small losses at 10 GHz. Another improvement could be the fitting of a dielectric stabiliser to the oscillator. Building a transmitter of this kind has not only the advantage of simplicity, having the 10 GHz source directly at the parabolas focus avoids losses in waveguides, coaxial lines, transitions, relays and so on. This would be particularly interesting in a receiver. The preamplifier could be built directly at the parabolas focus, the dish being illuminated by a small microstrip antenna etched next to the preamplifier (Fig.10).

As we know, any loss between the antenna and the preamplifier severely affects the receivers noise factor. An assembly like the one in Fig.11a should be much less lossy than, say, the one shown in Fig.11b, and much cheaper too.

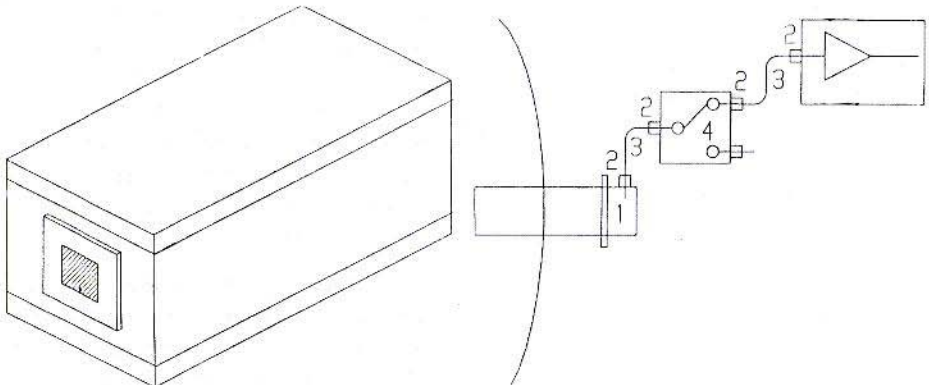


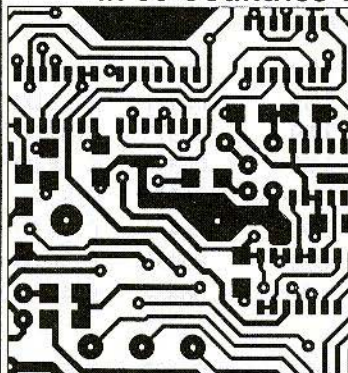
Fig.11a: The Preamplifier can be enclosed in its shielding box with a small Microstrip element glued on the outside. The assembly is placed in front of the Parabola with the Microstrip patch at the Focus.

Fig.11b: A more conventional and lossy setup.



EASY-PC, Schematic and PCB CAD

Over 19,000 Installations
in 80 Countries World-wide!

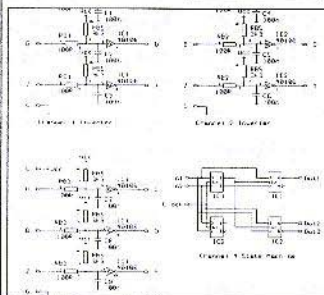


- Runs on:- PC/XT/AT/286/386/486 with Hercules, CGA, EGA or VGA display and many DOS emulations.
- Design:- Single sided, Double sided and Multi-layer (8) boards.
- Provides full Surface Mount support.
- Standard output includes Dot Matrix / Laser / Ink-jet Printer, Pen Plotter, Photo-plotter and N.C. Drill.
- Tech Support - free.
- Superbly easy to use.

Still
Only
£98.00!

Plus P&P+VAT

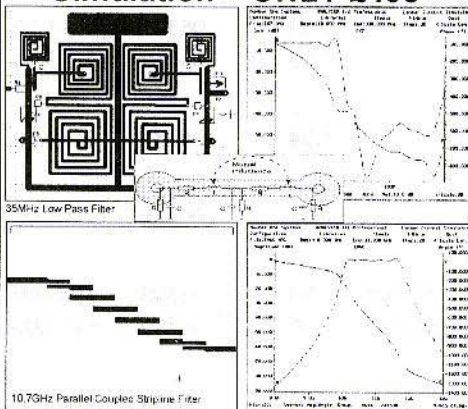
BRITISH
DESIGN
AWARD
1989



Options:-500 piece Surface Mount Symbol Library £48,
1000 piece Symbol Library £38, Gerber Import facility £98.

Electronic Designs Right First Time?

LAYAN - Electro-magnetic Simulation ONLY £495



Affordable Electronics CAD

LAYAN: New Electro-magnetic layout Simulator. Include board parasitics in your Analogue simulations. Links with and requires EASY-PC Professional XM and ANALYSER III Professional	\$950	£495
EASY-PC Professional: Schematic Capture and PCB CAD. Links directly to ANALYSER III, LAYAN and PULSAR	From \$375	£195
PULSAR: Digital Circuit Simulator	From \$195	£98
ANALYSER III: Analogue Linear Circuit Simulator	From \$195	£98
FILTECH: Active and Passive Filter Design program	From \$275	£145
STOCKIT: New comprehensive Stock control program for the small or medium sized business	\$275	£145
EASY-PC: Entry level PCB and Schematic CAD	\$195	£98
Z-MATCH for Windows: Windows based Smith-Chart program for RF Engineers.	\$475	£245

We operate a no penalty upgrade policy.
US\$ prices include Post and Packing
Sterling Prices exclude P&P and VAT.

For full information, please write, phone or fax:-

Number One Systems

UK/EEC: Ref. VHFCOM, Harding Way, St. Ives, Cambridgeshire., ENGLAND, PE17 4WR.

Telephone UK: 01480 461778 (7 lines) Fax: 01480 494042

USA: Ref. VHFCOM, 126 Smith Creek Drive, Los Gatos, CA 95030

Telephone/Fax: (415) 968-9306

e-mail: sales@numberone.com

International +44 1480 461778



ads43/4

COMPLETE KITS

for projects featured in VHF Communications

KIT	DESCRIPTION	ISSUE	ART No	PRICE
DB1NV-006	Spectrum Analyser IF Amplifier	2/89	06370	£142.00
DB1NV-007	Spectrum Analyser Lo-PLL	2/89	06371	£ 62.00
DB1NV-008	Spectrum Analyser Crystal Filter	3/89	06372	£108.00
DB1NV-009	Spectrum Analyser Sweep Gen	3/89	06373	£ 48.00
DB1NV-010	Spectrum Analyser Digital Store	3&4/91	06378	£132.00
DB1NV-011	Spectrum Analyser Tracking Gen	2/92	06474	£143.00
DB1NV-012	Spectrum Analyser VCO 1450 MHz	4/92	06483	£ 39.00
DB1NV-013	Spectrum Analyser VCO 1900 MHz	4/92	06484	£ 41.00
DB6NT-001	Measuring Amp up to 2.5 GHz	4/93	06382	£ 60.00
DB6NT-002	Frequency Divider to 5.5 GHz	4/93	06383	£100.00
DJ8ES-001	23cm FM ATV Converter	1/91	06347	£ 93.00
DJ8ES-002	Digital Frequency Indicator	1/91	06352	£ 53.00
DJ8ES-003	IF Amplifier	1/91	06355	£ 55.00
DJ8ES-004	Demodulator	1/91	06362	£ 72.00
DJ8ES-019	Transverter 144/28 MHz	4/93	06385	£143.00
DJ8ES-019mod	Transverter 50/28 MHz	2/95	06392	£143.00
DJ8ES-020	Hybrid Amplifier for 144 MHz	1/94	06387	£179.00
DJ8ES-021	13cm FM ATV Exciter	2/94	06388	£ 67.00
DJ8ES-022	28/432 MHz Transverter Oscillator	2/95	06395	£ 59.00
DJ8ES-023	28/432 MHz Transverter Converter	2/95	06396	£114.00
DC8UG-007	5W PA for 13cm	3/94	06938	£286.00

Minimum postage and packing charge is £6.75. Credit Card orders +5%.

KM Publications, 5 Ware Orchard, Barby, Nr.Rugby, CV23 8UF, U.K.

Tel: (0)1788 890365

Fax: (0)1788 891883



KITS and PRINTED CIRCUIT BOARDS

for the Matjaz Vidmar GPS/GLONASS Receiver project

KITS

Name	Issue	Description	Art.No	Price
S53MV001	1/95	GPS RF Module	06491	£ 24.35
S53MV002/003	1/95	GPS Converter, Multiplier & Mixer	06493	£ 62.95
S53MV004	1/95	GLONASS RF Module	06494	£ 29.65
S53MV005	1/95	GLONASS IF Converter	06496	£ 43.95
S53MV006	1/95	GLONASS PLL Synth. Converter	06498	£ 19.15
S53MV007	2/95	GLONASS Synthesiser	06500	£ 22.95
S53MV008	2/95	GPS/GLONASS Second IF	06502	£ 14.40
S53MV009	2/95	GPS/GLONASS DSP Module	06504	£ 75.40
S53MV010	3/95	GPS/GLONASS CPU Board	06547	£ 194.55
S53MV011	3/95	GPS/GLONASS 8-key Keyboard	06549	£ 34.90
S53MV013	3/95	GPS/GLONASS PSU and Reset	06553	£ 20.60
BSGPS		Complete GPS Kit	06555	£ 410.00
BSGLONASS		Complete GLONASS Kit	06556	£ 425.00

PC BOARDS

Name	Issue	Description	Art.No	Price
S53MV001	1/95	GPS RF Module	06490	£ 9.60
S53MV002/003	1/95	GPS Converter, Multiplier & Mixer	06492	£ 10.05
S53MV004	1/95	GLONASS RF Module	06495	£ 9.60
S53MV005	1/95	GLONASS IF Converter	06497	£ 10.05
S53MV006	1/95	GLONASS PLL Synth. Converter	06499	£ 19.15
S53MV007	2/95	GLONASS Synthesiser	06501	£ 22.95
S53MV008	2/95	GPS/GLONASS Second IF	06503	£ 6.25
S53MV009	2/95	GPS/GLONASS DSP Module	06505	£ 25.80
S53MV010	3/95	GPS/GLONASS CPU Board	06548	£ 25.80
S53MV011	3/95	GPS/GLONASS 8-key Keyboard	06550	£ 6.75
S53MV013	3/95	GPS/GLONASS PSU and Reset	06554	£ 8.65
LPGPS		Complete set of GPS Boards	06557	£ 83.10
LPGLONASS		Complete set of GLONASS Boards	06558	£ 124.75

Minimum postage and packing charge is £6.75. Credit Card orders +5%.

KM Publications, 5 Ware Orchard, Barby, Nr.Rugby, CV23 8UF, U.K.

Tel: (0)1788 890365

Fax: (0)1788 891883

PRINTED CIRCUIT BOARDS

for projects featured in VHF Communications

DB1NV	Spectrum Analyser			Art No.	
PCB	DB1NV-006	IF Amplifier	Ed.2/89	06997	£ 17.25
PCB	DB1NV-007	Lo-PLL	Ed.2/89	06995	£ 17.25
PCB	DB1NV-008	Crystal Filter	Ed.3/89	06998	£ 17.25
PCB	DB1NV-009	Sweep Generator	Ed.3/89	06996	£ 17.25
PCB	DB1NV-010	Digital Store	Ed.3&4/91	06477	£ 21.15
PCB	DB1NV-011	Tracking Generator	Ed.2/92	06479	£ 15.50
PCB	DB1NV-012	VCO 1450 MHz	Ed.4/92	06480	£ 16.35
PCB	DB1NV-013	VCO 1900 MHz	Ed.4/92	06481	£ 16.35
DB6NT	Measuring Aids for UHF Amateurs			Art No.	ED. 4/93
PCB	DB6NT-001	Measuring Amp up to 2.5 GHz		06379	£ 17.75
PCB	DB6NT-002	Frequency Divider to 5.5 GHz		06381	£ 17.75
DJ8ES	23cm FM-ATV Receiver			Art No.	ED. 1/91
PCB	DJ8ES-001	Converter		06347	£ 10.75
PCB	DJ8ES-002	Digital Frequency Indicator		06350	£ 9.65
PCB	DJ8ES-003	IF Amplifier		06353	£ 7.95
PCB	DJ8ES-004	Demodulator		06356	£ 10.30
DJ8ES	28/144 MHz Transverter			Art No.	ED. 4/93
PCB	DJ8ES-019	Transverter 144/28 MHz		06384	£ 17.75
PCB	DJ8ES-020	Hybrid Amplifier 144 MHz		06386	£ 17.25
DF9PL	High Stability Low Noise PSU			Art No.	ED. 1/93
PCB	DF9PL-001	30 Volt PSU		06378	£ 9.80
PCB	DF9PL-002	Pre-Stabiliser		06376	£ 10.20
PCB	DF9PL-003	Precision Stabiliser		06377	£ 11.20
F6IWF	10 GHz FM ATV Transmitter			Art No.	ED. 2/92
PCB	F6IWF-001	DRO Oscillator - PTFE		06485	£ 16.20
PCB	F6IWF-002	Modulator and Stabiliser		06486	£ 12.00
DC8UG	13cm GaAsFET PA			Art No.	ED. 3/94
PCB	DC8UG-PA	5W PA for 13cm		06936	£ 19.25
PCB	DC8UG-NT	Power Supply for the PA		06937	£ 7.75

Minimum postage and packing charge is £6.75. Credit Card orders +5%.

KM Publications, 5 Ware Orchard, Barby, Nr.Rugby, CV23 8UF, U.K.

Tel: (0)1788 890365

Fax: (0)1788 891883



VHF COMMUNICATIONS

A Publication for the Radio Amateur Worldwide

Especially Covering VHF, UHF and Microwaves

Volume No. 27 . Winter . Edition 4/1995

Publishers

KM PUBLICATIONS,
5 Ware Orchard, Barby, Nr. Rugby,
CV23 8UF, United Kingdom
Tel: 01788 890365
Fax: 01788 891883

Internet:
vhf-comm@g6iqm.demon.co.uk

Compuserve: 100441377

Editor

Mike Wooding G6IQM

VHF COMMUNICATIONS

The international edition of the German publication UKW-Berichte is a quarterly amateur radio magazine, especially catering for the VHF/UHF/SHF technology. It is owned and published in the United Kingdom in Spring, Summer, Autumn and Winter by KM PUBLICATIONS.

The 1995 subscription price is £15.00, or national equivalent. Individual copies are available at £4.00, or national equivalent each. Subscriptions should be addressed to the national representative shown in the next column. Orders for individual copies of the magazine, back issues, kits, binders, or any other enquiries should be addressed directly to the publishers.

NOTICE: No guarantee is given that the circuits, plans and PCB designs published are free of intellectual property rights. Commercial supply of these designs without the agreement of the Author and Publisher is not allowed. Users should also take notice of all relevant laws and regulations when designing, constructing and operating radio devices.

© KM PUBLICATIONS

All rights reserved. Reprints, translations, or extracts only with the written approval of the publishers

Translated by: Inter-Ling Services,
62 Caldecott Street, Rugby,
CV21 3TH, UK

Printed in the United Kingdom by:
Cramphorn Colour Printers Ltd.,
15c Paynes Lane, Rugby.

AUSTRIA - Verlag UKW-BERICHTe, Terry D. Bittan, POB 80,
D-91081 BAIERSDORF, Germany. Tel: (9133) 47-0
Fax: 09733 4747 Telex: 629 887. Postgiro Nbg. 30445 858.

AUSTRALIA - W.I.A., P.O. Box 300, SOUTH CAULFIELD,
3162 VIC, Australia. Tel: 528 5962

BELGIUM - UKW-BERICHTe, POB 80, D-91081 BAIERSDORF,
Germany. Tel: (9133) 47-0. Fax: 09733 4747 Telex: 629 887.
Postgiro Nbg. 30445 858.

DENMARK - KM PUBLICATIONS, 5 Ware Orchard, Barby,
Nr. RUGBY, CV23 8UF, UK. Tel: +44 788 890365.
Fax: +44 788 891883. Email: vhf-comm@g6iqm.demon.co.uk

FRANCE - Christianne Michel F5SM, SM ELECTRONIC, 20bis
Avenue des Clairons, F-89000 AUXERRE, France
Tel: (86) 46 96 59

FINLAND - KM PUBLICATIONS, 5 Ware Orchard, Barby,
Nr. RUGBY, CV23 8UF, UK. Tel: +44 788 890365.
Fax: +44 788 891883. Email: vhf-comm@g6iqm.demon.co.uk

GERMANY - UKW-BERICHTe, POB 80, D-91081
BAIERSDORF, Germany. Tel: 09133 7798 0.
Fax: 09133 779833. Postgiro Nbg. 30445 858.

GREECE - C+A ELECTRONIC, P.O. Box 25070, ATHENS
100 26, Greece. Tel: 01 52 42 867. Fax: 01 52 42 537

HOLLAND - KM PUBLICATIONS, 5 Ware Orchard, Barby,
Nr. RUGBY, CV23 8UF, UK. Tel: +44 788 890365.
Fax: +44 788 891883. Email: vhf-comm@g6iqm.demon.co.uk

ITALY - ADB ELETTRONICA di Luchesi Fabrizio IW5ADB,
Via Vecchia Romana 266, 55100 ANTRACCOLI, (LUCCA), Italy.
Tel: 0583 952612. Fax: 0583 91109

NEW ZEALAND - Judith Holland, AUCKLAND VHF GROUP
Inc., P.O. Box 10 138, AUCKLAND 1030, New Zealand.
Tel: 0 9 480 1556

NORWAY - HENNING THEG RADIO COMMUNICATION
LA4YG, Kjolaveien 30, 1370 ASKER, Norway.
Postgirokont: 3 16 00 09

SOUTH AFRICA - HI-TECH BOOKS, P.O. Box 1142,
RANDBURG, Transvaal 2125, South Africa. Tel: (011) 465 3385

SPAIN & PORTUGAL - JULIO A. PRIETO ALONSO EAMC,
Donoso Cortes 38 5º -B, MADRID 15, Spain. Tel: 543 83 84

SWEDEN - WAVELINE AB, Box 60224, S-210911 MALMÖ,
Sweden. Tel: 40 16 42 66. Fax: 40 15 05 07. GSM: 0705 16 42 66
Postgiro: 13 78 93 - 4

SWITZERLAND - KM PUBLICATIONS, 5 Ware Orchard, Barby,
Nr. RUGBY, CV23 8UF, UK. Tel: +44 788 890365.
Fax: +44 788 891883. Email: vhf-comm@g6iqm.demon.co.uk

UNITED KINGDOM - KM PUBLICATIONS, 5 Ware Orchard,
Barby, Nr. RUGBY, CV23 8UF, UK. Tel: +44 788 890365.
Fax: +44 788 891883. Email: vhf-comm@g6iqm.demon.co.uk

U.S.A. - WYMAN RESEARCH Inc., RR#1 Box 95, WALDRON,
Indiana 46182, U.S.A. Tel: (317) 525 6452

- Henry Rub, ATVQ MAGAZINE, 3 North Court Street,
Crows Point, Indiana 46307, U.S.A. Tel: (219) 662 6395.
Fax: (219) 662 6991

ELSEWHERE - KM PUBLICATIONS, address as for the U.K.

ISSN 0177-7505

**NOW AVAILABLE FROM MAINLINE
ELECTRONICS**

**TIMES MICROWAVE SYSTEMS LMR™
COAXIAL CABLES**



**AMONGST THE FINEST MONEY
CAN BUY**

Type No.	Centre Conductor &	Diameter	Loss per 100m	
			30 MHz	2000 MHz
LMR-200	Bare Copper	1.12mm	5.91dB	49.3dB
LMR-400	Copper Clad Aluminium	2.77mm	2.30dB	19.7dB
LMR-600	Copper Clad Aluminium	4.47mm	1.38dB	12.8dB
LMR-1200	Copper Tube	8.86mm	0.69dB	4.91dB

Enquire for delivery, latest prices and full specifications
Other types of cable from the range available to order

Mainline Electronics

P.O. Box 235, Leicester, LE2 9SH, UK

Tel: (0)116 278 0891

Fax: (0)116 247 7551